THE DEVELOPMENT OF THUNDERSTORM COMPLEXES AND THEIR ASSOCIATED VERTICAL TRANSPORTS

by

GARY LEE MELVIN
B.S., Saint Louis University
(1967)

SUBMITTED IN PARTIAL FULFILLMENT
OF THE REQUIREMENTS FOR THE
DEGREE OF
MASTER OF SCIENCE
at the
MASSACHUSETTS INSTITUTE OF TECHNOLOGY
August, 1968

Signature of Author...
Department of Meteorology, 19 August 1968

Certified by...
Thesis Supervisor

Accepted by...
Chairman, Departmental Committee on Graduate Students

THE DEVELOPMENT OF THUNDERSTORM COMPLEXES AND THEIR ASSOCIATED VERTICAL TRANSPORTS

by

GARY LEE MELVIN

Submitted to the Department of Meteorology
on 19 August 1968
in partial fulfillment of the requirements
for the degree of
Master of Science

ABSTRACT

Radar observations and a simple cell model have been employed to examine the relationship between the precipitation in convective cells and the associated lighter precipitation within seven thunderstorm complexes. It has been hypothesized that the lighter precipitation in the complex is a result of divergence of condensate produced within convective elements rather than a result of lifting on a larger scale. The observed characteristics of the areas have been described. The amounts of precipitation deposited by the convective cells and the surrounding complex and the average vertical velocities necessary to produce these amounts have been computed. The results were consistent with the hypothesis.

The latent heat released within the convective cells and the vertical transports of mass and momentum were computed for the seven thunderstorm complexes. The release of latent heat and downward momentum transport appear sufficiently large to warrant further investigation as to their effect upon larger circulations.

Thesis Supervisor: Dr. Pauline M. Austin
Title: Research Associate

ACKNOWLEDGMENTS

I would like to thank Dr. Pauline M. Austin for her valuable advice and never-ending patience, Professor James M. Austin for his comments and constructive criticisms of the paper, and my wife, Irene, for her help in preparation of the figures and tables and edifying encouragement.

TABLE OF CONTENTS

LIST OF FIGURES

LIST OF TABLES

I. INTRODUCTION

The thunderstorm, with its associated heavy rainfall, strong surface winds, large hailstones, and tornadoes, has fascinated meteorologists, not only as an extreme weather hazard, but as a rebuff to explanation. Rapid time changes and remarkably sharp small-scale spatial variability have precluded adequate observational evidence from which a general theory of thunderstorm evolution might have been established. Although thunderstorm dynamics have yet to be totally explained, a more than rudimentary knowledge of such small-scale atmospheric convection does exist. Observation has established that thunderstorms are typically a complex of several units each consisting of an updraft with its associated convergence-divergence pattern, hydrometeors, and downdraft. These units have lifetimes less than that of the storm (Byers and Braham, 1949). In addition, these storms are observed to occur as a scattered, isolated phenomenon or in a group, lying in a line.

This knowledge has been gained, in part, through the application of radar to meteorological research. With its ability to quantitatively map the three dimensional liquid water content of the atmosphere, radar furnishes information about the structure and intensity of thunderstorm activity. The ability to sample over a large volume in a short time period renders radar an essential observational instrument for observing a storm throughout its entire lifetime. However, its resolution is marginal for depicting the internal structure of thunderstorms. It is necessary to define the components of these convective storms on the basis of what the radar sees in order to discuss them meaningfully, even though the definitions may be somewhat arbitrary. A cell is defined as a very small echo close to the limit of the radar's resolution. Generally, the cell echo appears a high signal intensity level and is surrounded by a small area (on the order of 10^2 to 10^3 mi.^{2}) of less intense echo. A cluster of these cells, occurring either simultaneously or in a sequence, is defined as a complex. Any group of these complexes which appear on the radar as a line is defined as a squall line.

Previous radar investigations of New England thunderstorms (Boucher and Wexler, 1961, Swisher, 1959, Cochran, 1961, Stem, 1964, and Omotoso, 1967) have recognized that they do appear as complexes composed of small intense echoes surrounded by larger areas of lesser intensity. The studies described the characteristics such as size, duration, and motion of the various precipitation areas. No attempt was made to determine whether the lighter precipitation, which was continuously observed to accompany the intense cores, was condensed within the cells or produced by some other mechanism such as a small-scale convergence-divergence system.

An understanding of the relationship between precipitation areas of various sizes as observed by the radar, is important not only in studies of mesoscale circulations and precipitation physics, but also is critical in determining the associations between global, synoptic, and sub-synoptic circulations. Two features of the small-scale motions which may be significant to the larger ones are the release of latent heat and the vertical transport of such quantities as momentum, sensible heat, and moisture. Austin (1968) has suggested that these relationships can be studied from quantitative radar observations and a simplified cell model wherein the vertical mass transport of air is related to the total amount of precipitation produced by the convective motions. It is, therefore, necessary to determine how much of the precipitation within the is actually produced within the cells or is produced by some other mechanism such as a mesoscale convergence-divergence system.

The purpose of this study is to investigate the development of the thunderstorm complex in an attempt to clarify the relationship between convective cells and associated lighter precipitation. The hypothesis that the lighter precipitation is produced within the convective elements and diverged to a broader area will be examined. In addition, latent heat release and vertical transport of momentum will be computed in order to obtain an estimate of their magnitudes.

II. THE THUNDERSTORM MODEL

It is customary to model the behavior of the air and water substance throughout the evolution of the thunderstorm using the results of explorations in an attempt to ascertain what actually takes place. Excellent review articles (Severe Local Storms, Meteorological Monographs, 1963) are available, and it is not necessary to consider present thunderstorm models in detail. However, certain thunderstorm characteristics are common to most models and are generally felt to be realistic, while others are assumed with varying degrees of confidence.

Outward physical characteristics of thunderstorm complexes are obviously the least disputed. Cells range from less than a mile to a maximum of four or five miles in diameter. Complexes have a horizontal dimension from ten to fifty miles. Cells range in height from 25,000 feet to greater than 50,000 feet and possess lifetimes which average 20 minutes. Small echoes, here defined as cells, move with the mean wind in the middle troposphere (Byers and Braham, 1949, and Ligda, 1953). The motion of the complex, which consists of propagation due to new cell growth as well as movement with the wind currents, may be with or to either side of the mean tropospheric wind, but most often is to the right and slower (Byers, 1942, and Newton and Katz, 1958).

Modelling the internal structure of a convective cell requires that certain assumptions be made that are based upon less than sufficient direct observational evidence. An updraft must exist to produce precipitation. The characteristics of an updraft include the magnitude of the vertical velocity and its variation with height, draft dimension and lifetime, the amount and effect of entrainment into the draft, and the ratio of total water condensed in the updraft to that deposited as precipitation. It requires an extensive observational network, such as that used by the Thunderstorm Project (Byers and Braham, 1949), to observe these characteristics.

As was demonstrated by Kessler (1967) and formulated into a model by Austin (1968), the total amount of lifting produced by an updraft within a convective cell must be related to the total observed precipitation from that cell. Since radar yields the intensity, dimensions, and duration of a precipitation area, the total amount of precipitation can be determined. Those aspects of an updraft which are of particular importance in a model designed to determine vertical transports from observed precipitation are the variation of vertical velocity with height, the amount and effect of entrainment into the updraft, and the ratio of total water condensed to that actually deposited as precipitation.

Fairly realistic approximations to updraft profiles are either linear or parabolic (Atlas, 1966, and Kessler, 1967). As air rises in the updraft, lateral mixing will occur to maintain mass continuity. The process and its effect have been discussed in detail. Stommel (1947) introduced the concept of entrainment to account for cloud temperatures observed to be less than calculated in a parcel ascent. The drawing of unsaturated air through the sides of a cloud results in partial evaporation of the liquid water content. This and the mixing of cooler air from outside the cloud will cause a rising parcel to cool at a rate greater than the moist adiabatic. Austin (1948) demonstrated that in-cloud lapse rates and cloud height are highly sensitive to entrainment rate and the environmental dryness. Houghton and Cramer (1951) showed that if there is buoyancy, entrainment is necessary to satisfy mass continuity. With an updraft of constant cross section, entrainment in the convergent region below the level of maximum vertical velocity and loss through divergence above that level are determined by the shape of the vertical velocity profile.

The cumulus convection which precedes the development of thunderstorm complexes occurs in unsaturated air which is drawn into the updrafts by the necessary entrainment process. This lateral mixing of drier air from the environment into the ascending air of a cumulus cloud reduces the degree of instability within it. If the initial buoyancy is great enough, the cumulus cloud may develop into a thunderstorm.

Often a thunderstorm initially appears on the radar as a very small echo of high intensity. This echo soon becomes surrounded by a larger area of lighter precipitation. As subsequent cells appear, the area of lighter precipitation continues to grow and reaches a maximum horizontal dimension many times that of a single cell. Some models of convective cells have failed to recognize this area of lighter precipitation and entrain unsaturated environmental air into the updrafts. Considering the necessary pre-thunderstorm convection and the ultimate size of thunderstorm complexes, it seems reasonable to consider the cells as growing and operating within a saturated environment after some initial growth period. As stated in the previous paragraph, it is recognized that the original cumulus convection takes place in an unsaturated environment. Probably, the cell initially detected by the radar is also operating in a less than saturated environment.

As convection and condensation proceed precipitation develops, but not all of the condensate is actually deposited as rain. Some may be left as could, evaporated from cloud sides, or evaporated in a downdraft. Braham (1952) has provided estimates of the percentages of condensate lost to these various sinks. The importance of these estimates and the manner in which they are applied to the model are discussed in subsequent chapters.

Those characteristics of an updraft important in a model designed to relate vertical mass transport to observed amounts of precipitation have been discussed. This model, which is outlined in the following chapter, is used to obtain estimates of latent heat release and the transport of momentum. Since the observed precipitation is the basis of the computations, it is important to know whether this precipitation was produced by stratiform or convective lifting.

For a given amount of condensate a fixed amount of latent heat is released, but the manner in which the air is lifted to cause the condensation determines where this heat will be deposited. In stratiform lifting, the heat is deposited in the layer where condensation occurs. However, the great vertical extent and large vertical velocities of the thunderstorm deposit the latent heat condensed in the updrafts near the top of the cells.

The mode of lifting is especially important in vertical transports. The air lifted within a narrow convective cell is lifted rapidly and drawn from all levels below the level of maximum vertical velocity. Thus, air entrained from the lowest layers has the opportunity to be lifted to the top of the thunderstorm cell. In stratiform lifting, the vertical velocities are not great enough to carry air through a very deep layer. If the air lifted within a convective cell conserves its characteristics during the ascent, the thunderstorm becomes a means of transporting quantities such as momentum through a deep layer.

It is necessary to know whether the light precipitation within the complex is produced within the convective cells or by stratiform lifting throughout the precipitation area in order to apply the model and compute the vertical transports and assess the effects of latent heating. Therefore, it is hypothesized that the lighter precipitation is a result of the divergence to the surrounding area of condensate produced within the convective cells. This hypothesis will be tested by determining the relative amounts of precipitation deposited by the cells and the complex excluding the cells and the average vertical velocities necessary to produce these observed amounts of precipitation, and by examining the physical characteristics of the precipitation areas. The data and methods of analysis appear in the following chapter.

III. DATA AND METHODS OF ANALYSIS

A. Data

The basic data utilized in this investigation consist of radar observations and conventional synoptic reports. The radar data were supplied by the Weather Radar Project located at the Massachusetts Institute of Technology and were in the form of 35 mm photographs of averaged, range-normalized signals, quantized into levels of 5 db. This corresponds to a factor of two in equivalent rainfall rate. This rate is obtained with the use of the empirical relationship: $Z = 200R^{1.6}$. Z is the radar reflectivity factor expressed in $mm^6\ m^{-3}$ and R is rainfall rate in $mm\ hr^{-1}$. Austin and Geotis (1960) estimate that the accuracy of the radar measurements is within 2-3 db or less than a factor of 2 in equivalent rainfall rate. The data were from the SCR-615-B which is a 10.7 cm radar having a beam width of 3 degrees between half power points. Because of an increase in sensitivity of the radar effected in the fall of 1964, data were chosen from 1965. The plan position observations were taken at an elevation angle of one degree and a range of 120 statute miles.

A careful examination of all data for the summer of 1965 was undertaken, and seven thunderstorm complexes were selected as a basis for computations. In all cases but one these storms were chosen because radar data, including both plan position and range-height indications, were available for the entire storm period. The seventh case was chosen because it involved the initiation and growth of a squall line within radar range.

Conventional synoptic data yielded the atmospheric conditions within which the storms were occurring. Raingauge records were examined, but the isolated nature of the majority of the storms made the reports of little use except to indicate the presence or absence of widespread light precipitation not detected by the radar. Examples of the data are given in Figures 7 through 10, and 16 through 37.

B. Analysis

The analysis detailed below was performed on six of the seven cases chosen. It was only slightly modified for the case where the squall line formed within radar range, because records were not available for its entire lifetime.

Information which is directly available from radar data consists of cell and complex echo duration, dimension, movement, precipitation rate, and total water deposit. The number of cells and their trajectories were determined by placing the PPI films upon a viewer which displayed each frame in sequence, allowing accurate tracking. An average of .05 hours was required for each frame, therefore, a complete sequence of intensity levels could be taken within 2-3 minutes. Thus, the rapid changes which occur within a complex could be viewed with a fair amount of accuracy.

Complex duration includes the time between the first appearance of a radar echo, associated with the first cell in the complex, and the disappearance of the complex echo. Cells first appear on the PPI as very small echoes near the upper limit of the radar's resolution. These spots generally increase in size while remaining at about the same intensity. Then, presumably with the termination of the updraft, the areas slowly continue increasing in size but decrease in intensity until reaching the same intensity level or precipitation rate as the complex. The lifetime of a cell is considered to include the time between the first appearance of the small spot and its loss of identity within the complex.

An average cell was determined for each complex by averaging the duration, dimension, and precipitation rate of all cells observed within the complex. The precipitation rate for a given cell was taken to be the average of those intensities which were indicative of it while it was in existence. The total water deposited by an average cell was then determined.

The total water deposited by the precipitation from the complex excluding the cells was computed by a lengthy process of determining the area corresponding to each intensity level for each sequence of PPI photographs. Since the time required to photograph the sequence was known the water deposited during that 2-3 minute interval could be computed. The sum of the values obtained from each series of PPI photographs equalled the amount deposited by the complex outside of the cells.

A comparison was then made between the amounts of precipitation deposited by the cells within a complex and that around the cells in order to determine whether the magnitudes were such that the amounts outside the cells could have been reasonably produced by condensation within the cells. The relationship between these precipitation amounts was then compared from storm to storm in order to determine its variability.

The model described below, after Austin (1968), was then applied to these observed amounts of precipitation to determine the mass transport necessary to produce them. In the model it is assumed that a linear updraft starts from an initial disturbance near the bottom of an unstable layer (Figure 1). As the initial air rises, equal amounts of air are entrained from each layer below z_1, the level of maximum vertical velocity. Likewise, equal amounts are lost to each layer above z_1 as the air velocity approaches zero at z_2. It is further assumed that the updraft has a uniform and constant cross section, and that air density remains constant with height. For computations, air density was taken to be 1 kg m^{-3}. Entrained air mixes thoroughly within the updraft, and the moisture condensed for every cubic meter of air which rises through z_1 is given by Austin as:

$$\left(\frac{1}{z_1-z_0}\right) \int_{z_0}^{z_1} [q_1(z) - q'(z)]dz + \left(\frac{1}{z_2-z_1}\right) \int_{z_1}^{z_2} [q'(z_1) - q'(z)]dz \quad (1)$$

where q(z) is the mixing ratio at any level z and the primed quantities refer to conditions within the updraft. For a given storm, q(z) can be obtained from radiosonde data.

Austin does not include a consideration of the surrounding precipitation of the complex in the cell model, but simply assumed that environmental air is entrained into the updraft. Since the complex is consistently associated with the cells in radar observations, it must be considered in a realistic cell model. It is proposed that the precipitation within the complex is a result of condensate produced within cell updrafts. The temperature within the complex is assumed to be the same as that within the environment, but the complex is saturated by condensate from the cells. The lapse rate within the cells would lie between the environmental lapse rate and the moist adiabatic, but would differ only slightly from the environmental rate. If the temperature in the cells is only a few tenths of a degree warmer than the air in the complexes the necessary buoyancy will be provided. Thus, the temperatures within the complex and the cell can be approximated by the environmental lapse rate. Therefore, q'(z) and q(z) would be very nearly the same. The environmental saturated mixing ratio was used for q'(z) and q(z) and was approximated by an exponential function for integration of equation (1). (Figures 11 through 14).

Of the condensate produced in the updraft, some will remain as cloud, some will be evaporated from cloud sides, some will fall as precipitation, and some will evaporate in the downdraft. The evaporation within the downdraft can be neglected since the downward mass transport within the downdraft equals the upward mass transport within the updraft necessary to condense out the moisture which is subsequently evaporated. Braham (1952) estimated that for average air mass thunderstorms in the eastern United States the condensate evaporated from cloud sides and left as cloud is twice that which falls as precipitation. Kessler (1967) in his kinematic models of cells embedded in saturated air, found that the amount left as cloud was roughly one-third as large as that left as precipitation. In this study various percentages of condensate were assumed to be left as cloud or evaporated aloft in order to examine the differences in mass transports necessary to produce such amounts.

Equation (1) gives the amount of moisture condensed per cubic meter of air passing through z_1, when the updraft speed varies linearly with height. This, plus the observed total water deposit, yields the vertical mass transport of air necessary to produce the observed precipitation. At any level, the downward transport of air outside of the cells must equal the amount transported upward within the updraft. This downward transport is assumed to take place as a uniform downward shift outside of the complex, since downward motion within the complex would result in evaporation of the precipitation within the complex.

Computations with the assumption of a constant updraft and no entrainment result in double the amount of condensate produced for each cubic meter rising through z_1. A parabolic updraft profile requires less mass transport to produce a given amount of precipitation than does a linear profile but more transport than the constant updraft. Thus, it would seem that the assumption regarding the vertical velocity profile introduces an uncertainty of less than a factor of 2 into the computed mass transport (Austin, 1968).

Average vertical velocities were computed by dividing the necessary vertical mass transport to produce the observed precipitation by the duration of an average cell. This results in an admittedly questionable value since a constant vertical velocity does not act for the entire duration of a cell, and the updraft duration is not necessarily equal to the echo lifetime. However, the given mass transport must take place during the lifetime of the cell to produce the observed water; therefore, the values presented must be somewhat of a minimum estimate of the actual maximum vertical velocity. These estimates were compared to observed vertical velocities within convective clouds in order to see whether realistic values were obtained, even though it is assumed that all the observed precipitation was condensed within the cells.

Finally, the amount of released latent heat corresponding to the observed precipitation and the transport of momentum across the level of maximum vertical velocity were computed. It was assumed that equal portions of air were entrained at all levels below z_1. The wind profiles in Figures 33 through 37 were used to compute the horizontal momentum at each level, and it was assumed that the entrained air conserved this momentum during its ascent. The values obtained in these computations were examined to determine the significance of their magnitudes.

IV. STORM CASE DESCRIPTIONS

A. Case I and II, June, 1965

Synoptic Situation

The major feature of the June 9, 1965, upper air pattern was a moderately cold trough extending southward from the Hudson Bay area to the northern Great Lakes Region. A 500-mb low pressure center was located over James Bay, and the flow aloft over the New England area was from the southwest.

A surface low and frontal system were associated with the upper level trough. The low was located in northern Ontario. A cold front extending southward from this low moved through the Midwest during the afternoon and evening of June 8 and occluded in Canada during the early hours of June 9. At 0100 EST on June 9, the front was stationary in the extreme eastern Great Lakes Region, while the northern section moved much more slowly than during the previous day.

Two thunderstorm complexes, which formed in the warm moist air in advance of the front, were examined. The first occurred between 0915 and 1013 EST and was associated with a widely spaced line of thundershowers. This line passed through New England and was followed by isolated thunderstorms which occurred throughout the day. Montpelier and Burlington, Vermont, Albany, New York, Boston, Massachusetts, and Concord, New Hampshire, reported thunderstorms prior to the occurrence of the second complex examined 1837 to 2106 EST.

The 0700 EST sounding for Albany, New York, (Figure 7), seemed most representive of the air mass in which the storms occurred. The moisture and temperature structure indicated a good possibility of convective activity. Surface conditions at storm times are given in Figures 2 and 3.

General Description of the Storms

A widely spaced line of thundershowers oriented southwest - northeast was present on the radar when it was turned on at 0853 EST, June 9. The complex studied developed in this line at 0915 EST and lasted until 1013 EST. The first echo was associated with the initial cell. The complex formed about this cell and increased in size until the third and last cell in the complex developed. Then the complex decreased in size and did not appear after 1013 EST. The line moved from 340° at approximately 20 mph. The complex moved from 285° at 19 mph (Figure 15).

The complex consisted of 3 cells having an average lifetime of 28 minutes and cross sectional area of 2 km^2 (0.8 mi^2). This area was determined by averaging the areas of the cell during each frame of PPI photographs as it appeared according to the definition in Chapter I. The characteristics of the cells are given in Table 10. The new cells formed to the lower right; however, one was quite removed from the others (Figure 16). Cell heights were estimated from radiosonde data to be midway between the level where the buoyancy ceased, determined from a parcel ascent, and where the kinetic energy was depleted, determined on an energy diagram. The estimated height of 12 km (40,000 feet) was in agreement with RHI's taken through the line two hours later. The bases of the cells were considered to be at the lifting condensation level which was approximately 1 km above the surface.

The saturation mixing ratio profile (Figure 11) was determined from the sounding in Figure 7. The mean precipitation rate in the cells was 16 mm hr^{-1}. An average cell deposited 1.5×10^{10} gm of water, and the complex, excluding the cells, deposited 2×10^{11} gm of water. The precipitation rate within the complex ranged from 1 to 10 mm hr^{-1}. A total transport through the level of maximum updraft of $1.8 \times 10^{10} m^3$ of air per cell was necessary to produce the total observed precipitation assuming no added condensate for cloud and evaporation from cloud sides. Tables 18 and

19 summarize these values.

The second complex had a lifetime from 1837 EST to 2106 EST. Two cells formed initially and an area of lighter precipitation gradually evolved about the two until they combined to form the complex. It contained a total of 14 cells with an average lifetime of 24 minutes. The cells averaged 8 km^2 in cross section (3 $mi.^2$). The cell characteristics appear in Table 11. All new cells developed near the right rear of existing cells and moved in the general direction of the 700-mb winds. Cells forming in the right half of the complex had a more northerly trajectory, while those forming in the left half tended to move more southerly. Radiosonde (Figure 7) and RHI (Figure 20) indicated cell tops at 12 km (40,000 feet) and bases at 1 km.

The movement of the complex is shown in Figure 17 to be from 320° at about 9 mph. It is quite evident from examining Figures 17 and 18 and Table 2 that the movement was a result of upper level winds and propagation from new cell growth.

The same saturation mixing ratio (Figure 11) was used as in Case I for computations. An average cell had a precipitation rate of 68 mm hr^{-1} and deposited a total of 2.2 x 10^{11} gm of water. The precipitation rate in the complex, outside of the cells, ranged from 1 to 23 mm hr^{-1}. The complex outside of the cells deposited a total of 3.6 x 10^{12} gm of water. Thus, total water deposit required a vertical transport of air through z_1 equal to 1 x $10^{11} m^3$ of air per cell. (Tables 18 and 19)

B. Cases III, IV, V, and VI, June 23 and 24, 1965

Synoptic Situation

At 1300 EST. June 23, 1965, a surface wave, apparently associated with some disturbance aloft, appeared in the warm sector preceding a cold front. The front extended southward from a low in southeastern Quebec. This wave moved through New England in the early evening triggering a vigorous squall line. The 1900 EST sounding for Albany, New York, (Figure 8) revealed an unstable atmosphere with warm, very moist air at lower levels. The winds were southerly up to 850 mb and southwesterly changing to westerly above (Table 3). The surface analysis prior to storm time appears in Figure 4.

The cold front moved eastward throughout the night and reached Boston about 1100 EST. Radiosonde data at 0700 EST from Portland, Maine, indicated conditions in advance of the front. The atmosphere was highly conditionally unstable and very moist up to 300 mb (Figure 9). Winds were southwesterly at all levels. Skies were generally overcast from late afternoon on June 23 until noon on June 24. There was widespread precipitation from 1900 EST until midnight. After midnight the precipitation was much more scattered and generally ended by 1200 EST. The position of surface features are shown in Figure 5.

General Description of the Storms

Three complexes were chosen from the well developed squall line which appeared on the radar on the evening of June 23. The line was around 200 miles long and moved approximately 25 mph from 320° (Figure 23). The complexes chosen had lifetimes of 65, 25, and 75 minutes and all formed about the initial cell after that cell was detected by radar. The characteristics of the cells within these complexes are given in Tables 13, 14, and 15, while those of the complexes are given in Table 12. Figures 21 and 22 show storm and cell movements. The cells and complexes appeared to be moving with the winds at and above 700 mb (Table 3). The new cells seemed to build near the front of existing cells, but there was no preference as to the side on which they formed. Cell heights were estimated at 13 km (45,000 feet) with bases at 1 km (Figure 24).

The mean precipitation rate of cells in Case III was 31 mm hr^{-1}. Therefore, an average cell deposited 3.6×10^{10} gm of water during its 18 minute lifetime. The precipitation rate within the complex outside of the cells ranged from 1 to 20 mm hr^{-1}, and the complex deposited 3.9×10^{10} gm in addition to that deposited by the cells. Therefore, each cell transported 2×10^{10} m^3 of air to account for the total precipitation. The saturation mixing ratio shown in Figure 14 was used for these computations.

The average cell in Case IV had a lifetime of 15 minutes and a precipitation rate of 8.5 mm hr^{-1}. Thus, it deposited 5×10^9 gm of water. Precipitation rates in the surrounding complex ranged from 1 to 4 mm hr^{-1} and amounted to 5.4×10^{10} gm of additional water. 4.2×10^9 m^3 of air were transported vertically in each cell to produce the observed total precipitation.

Case V had three cells with an average lifetime of 25 minutes and mean precipitation rate of 20 mm hr^{-1}. Each cell deposited $3 \cdot 10^{10}$ gm of water. The precipitation rates within the complex ranged from 1 to 8.5 mm hr^{-1} and deposited a total of 3.3×10^{11} gm in addition to that deposited by the cells. The required vertical transport for each cell to produce the total observed precipitation was 2.6×10^{10} m^3.

A squall line began to form at 0958 EST on June 24, 1965, and the growth was followed until 1100 EST. The first cells appeared to the southwest of the radar site and subsequent growth was to the northeast. Figures 25 and 26 illustrate the development. In the beginning stages of the line development, the complexes would form about the cells sometime after their initial detection. After several cells had formed the complexes joined and the line became a combination of many cells and complexes (Figure 27). The characteristics of the cells which formed up to 1100 EST are given in Table 16. The cells for which a total lifetime is not given were in existence when observations were halted at 1100 EST. The cells moved slightly to the right of the 700-mb winds (Table 4). The average cell lifetime was 27 minutes and cross sectional area was 2 km^2 (0.8 $mi.^2$). Figure 28 shows cell heights near 9 km (30,000 feet). Cell bases were estimated to be at 1 km. There appeared to be no preferred regions of new cell growth.

The mean precipitation rate of an average cell was 21 mm hr^{-1} and such a cell deposited 1.9×10^{10} gm of water. The precipitation within the complex outside of the cells ranged from 1 to 15 mm hr^{-1}. The amount of water in the complex at the time when observations were halted was determined by the expression $Z = 0.083M^{1.82}$ (Barge, 1968). Thus, the precipitation up to 1100 EST in the complex outside of the cells plus the amount of precipitation remaining aloft within the complex at 1100 EST equalled 1.35×10^{12} gm. The total mass transport per cell to account for all observed precipitation was 5.7×10^{10} m^3.

C. Case VII, August 28, 1965

Synoptic Situation

Scattered air mass thunderstorms occurred within radar range of Boston on August 28, 1965. A surface low pressure center was located just northeast of the Great Lakes region having a complex frontal system associated with it. Extending eastward from the low into central Maine was a stationary front. Trailing southward from the low were two cold fronts (Figure 6). A secondary cold front managed to catch the primary in the late afternoon and system moved through Boston during the evening of August 28.

The storms occurred in a warm sector southeast of the low. The flow aloft changed from southerly to southwesterly in the late afternoon as a tight 500-mb trough moved through the area. A jet was located over the region of activity.

Radiosonde data at 1300 EST for Portland, Maine, Nantucket, Massachusetts, and Albany, New York, were remarkably similar. The atmosphere was conditionally unstable (Figure 10) and there existed a strong wind shear (Figure 37 and Table 5).

General Description of the Storm

The storm complex chosen had a lifetime from 1454 to 1652 EST. There were a total of 13 cells which formed in sequence within the complex. Cell characteristics are given in Table 16 and illustrated in Figure 26. The average duration of a cell was 20 minutes, and their average cross sectional area was 5 km^2. The movement of the complex is shown in Figure 25 to be from 240^o at approximately 33 mph. Cells extended through a layer from 1 to 11 km (35,000 feet). New cells appeared forward of existing cells (Figure 30), either to the right or left, or replacing the cells in the same path. Cells forming on the right of existing cells moved more easterly and cells forming on the left moved more northerly. Two cells appeared initially on the radar and complexes of lighter precipitation quickly formed about them. These two complexes joined to form the large one observed. The complex reached a maximum size of 330 km^2 and dissipated with the last cell in the complex.

The average cell had a precipitation rate of 60 mm hr^{-1} and deposited 1.9×10^{10} gm of water. The precipitation rate within the complex ranged from 1.5 to 42 mm hr^{-1}, and deposited 2.9×10^{12} gm of water in addition to that left by the cells. 5.7×10^{10} m^3 of air were transported vertically across z_1 in each cell to produce the total observed precipitation.

V. DISCUSSION OF RESULTS

A. Development of the Thunderstorm Complex

The physical characteristics of the seven thunderstorm complexes examined support the hypothesis that the complexes develop as a result of condensate, produced within the cells, being diverged to the surrounding atmosphere rather than by slow lifting and condensation throughout the area of precipitation. The most obvious fact observed in all cases was that the precipitation within the complex always developed about the cells. The movement of the complexes was a combination of propagation from new cell growth and movement with the mean tropospheric winds. The complexes developed after the detection of the cell echoes and terminated with the expiration of the final cell or cells. Thus, the lifetime of a complex is equal to the period during which cell echoes are apparent. In addition, complexes seem to increase in size to some maximum horizontal dimension at which they remain for the majority of their lifetime. RHI's indicate that the complexes have the same vertical development as the cells about which they occur. This strengthens the possibility of divergence from the cells producing the precipitation within the complex instead of some lifting mechanism on a scale larger than that within the cells (Figures 20, 24, and 32). Another interesting fact observed from RHI's taken nearly upwind (Figures 24 and 32) is that the precipitation aloft within the complex extends far downwind from the location of the cells. This fact lends considerable credence to the proposed hypothesis. In addition, Figures 19 and 31, show that the majority of the complex is located downwind of the cells within. In both cases a wind shear existed (Figures 34 and 37). Thus, the precipitation diverged aloft was being carried downwind. This shear may have contributed to the further development of the cells by removing mass aloft and redistributing warm moist air downwind of the storm.

The results of computations outlined in Chapter III appear in Tables 18 through 20. Table 18 presents the water deposit, latent heat release, and transports of mass and momentum across the level of maximum vertical velocity for an average cell from each complex. In computing these values, it was assumed that equal amounts of condensate were deposited as precipitation and left as cloud, but the surrounding precipitation in the complex was neglected. Table 19 summarizes the same quantities assuming that the cells produce all observed precipitation but no cloud or cloud evaporation. In addition, it relates the amounts of water deposited by the complexes, cells, and the complexes excluding the cells. Table 20 gives the average vertical velocity, across the level of maximum vertical velocity, necessary to produce the water deposited by the cells, the complexes, and various assumed additional percentages of observed total precipitation assumed to have been left as cloud or evaporated from cloud sides.

The most significant fact to be ascertained from Tables 18 and 19 is that in all cases but one the water deposited by the complex excluding the cells is within a factor of 2 or 3 of the sum of the water deposited by the cells within the complex. In no case is there an order of magnitude difference. Even though the number of cells within a single complex ranged from 3 to 14, the water deposited by the complexes excluding the cells was nearly equal to the amount deposited by all the cells. This surely indicates a close relationship between the cells and the precipitation in the complex. Even in Case VI, where the cells were made to account for all precipitation observed in the development of a squall line, the water deposited by the line excluding cells and that deposited by the cells differed by a factor of three.

It seems highly unlikely that the same relationship would be found if some other mechanism was responsible for the water deposited by the complex.

A comparison of the computed average vertical velocities and measured vertical velocities within thunderstorms also supports the hypothesis. The computed vertical transports and average vertical velocities depend upon the amount of condensate which is assumed to have been deposited as cloud and evaporated from cloud sides. Braham (1952) has provided estimates of the water budget of a thunderstorm based upon data obtained in the Thunderstorm Project. It is not clear, exactly, how these estimates would apply to this study because of differences in which precipitation was attributed directly to the cells. It seems that Braham divided total observed precipitation by the number of cells, thus having the cells produce all precipitation. In any event, his are the only estimates available which are based upon observation. Braham estimated that twice as much condensate would be left as cloud than would be deposited as precipitation. This may be somewhat of an overestimate in cases such as II, IV, and VII where there appeared a good number of cells. Braham's estimate was considered to be an upper limit on the amount of condensate left as cloud.

If it is assumed that equal amounts of condensate are deposited as precipitation and left as cloud (Austin, 1968), the necessary average vertical velocities are less than 20 mps in all cases. Four of the seven cases are then below 10 mps. If Braham's requirements are met, all cases are below 30 mps with five of the seven cases below 20 mps and three below 15 mps.

The Thunderstorm Project observed updraft speeds of 5 to 10 mps with maximums of 25 mps in 25,000 foot penetrations of thunderstorms in Ohio and Florida. Glider flights in Germany yielded values of 20 to 30 mps consistently

(Ludlam, 1963), while radar tracking of objects through the strongest portions of thunderstorm updrafts have estimated velocities at 17.5 to 27.5 mps (Battan, 1963). Thus, it seems that values such as those appearing in Table 20 are compatible with observation. Indeed, if Braham's values are an overestimate then the required velocities would appear quite realistic.

Processes contributing to the development of thunderstorm complexes may well be more complicated than the proposed "cell-source" origin of the precipitation outside of the cells. Mesoscale convergence-divergence systems, sea breezes, topography, and any other mechanism which creates upward motion may contribute to the formation of the precipitation manifest in the complex. But, observations of the physical characteristics of the complexes and the values in Tables 18, 19, and 20 indicate that the condensate produced within convective cells can well be and probably are the source of the precipitation in the complexes.

B. Computation of Vertical Transports

Tables 18 and 19 present the values computed for the release of latent heat and vertical transport of momentum. Table 18 presents these values for an average cell from each complex assuming that equal amounts of condensate were deposited as precipitation and left as cloud. The values in Table 19 were obtained assuming that the cells within the complexes produced only the observed precipitation from the entire complex. Thus, the values in Table 19 are a minimum estimate and would increase depending upon the additional amounts of condensate assumed to have been produced for cloud and cloud evaporation.

In large convective cells such as those observed in this study, latent heat is released from the cloud base to the cloud top and deposited by the updraft in the upper region of the storms. The substantial rate of condensation within the thunderstorm updrafts and the great vertical development suggest that the thunderstorm might play a significant role in the vertical transport of heat. The latent heat released in the seven storm cases studied ranged from 6.7×10^{11} kj to 1.7×10^{13} kj. A total of 3.5×10^{13} kj was released in all. The maximum heating rate, 2×10^{9} kj sec^{-1}, was accomplished in Case II. Tracton (1968) found a value of 6.2×10^{11} kj sec^{-1} in an extratropical cyclone. Considering the relative amounts of precipitation produced between the isolated thunderstorm complex and a widespread extratropical cyclone, a difference of two orders of magnitude in effective heating rates would suggest the thunderstorm may be an effective mechanism for localized heating from condensation.

From Table 19, it is seen that the thunderstorm appears to be a major mode of momentum transport. The values for transport of momentum across the levels of maximum vertical velocity, z_1, ranged from 9.2×10^{10} kg m sec^{-1} to 9.4×10^{12} kg m sec^{-1}. For the 1.4×10^{13} gm of precipitation which were observed to fall from the seven storms, there was a total downward transport of 2×10^{13} kg m sec^{-1}. It was assumed that the seven case storms occurred in atmospheres that were typical of thunderstorm activity in New England and the results of this study were applied to the 1×10^{16} gm of purely convective precipitation which are estimated to fall in an area of 4×10^{4} km^{2} about the radar site in one year (Austin, 1968). This yielded 1.4×10^{16} kg m sec^{-1} transported downward in one year. Computations of Starr and White (1951) indicate that the necessary downward transport of eastward momentum between 31° and 65° north latitude is 1.6×10^{5} gr cm sec^{-1} per cm^{2} per year. This is a requirement of 6.4×10^{16} kg m sec^{-1} for the 4×10^{4} km^{2} area per year. The estimated downward transport due to convective storms is nearly one-fourth of the required amount.

VI. CONCLUSIONS

An understanding of the relationship between precipitation areas within thunderstorm complexes is important in studies of mesoscale circulations, precipitation physics, and in determining the associations between synoptic and subsynoptic circulations. Radar observations and a simple cell model have been used to examine the relationship between precipitation within thunderstorm cells and the associated lighter precipitation surrounding them. It was hypothesized that the lighter precipitation is a result of the divergence of condensate produced within the cells in contrast to some mechanism, such as a mesoscale convergence-divergence system, creating precipitation outside of the cells.

The characteristics of the cells and complexes as observed by radar have been described. The lighter precipitation within the complexes develops about the cells, has a lifetime equal to the period when cells are apparent, moves with the cells, has the same vertical development as the cells, and can often be observed aloft and downwind of the cells.

The amount of water deposited as precipitation by the complex excluding the cells was found to differ in most cases by a factor of 2 or 3 and at most 4 from the water deposited by the cells within the complex. This close relationship was observed in all complexes regardless of the number of cells embedded within them. The same relationship was found to exist in a squall line whose development was observed.

The average vertical velocities necessary within the convective cells to produce the observed total amount of precipitation agree with observed updraft velocities. Even when the observed water deposit was tripled, to account for additional water sinks, the values were realistic.

The observed characteristics, the amounts of water deposited, and the computed average vertical velocities demonstrate that the convective cells can be the source of all the observed precipitation from a thunderstorm complex.

The latent heat released within the convective cells and the transports of mass and momentum were computed for the seven thunderstorm complexes employing a cell model wherein the vertical mass transport of air was related to the total observed precipitation. The latent heat release and downward momentum transport appear to be sufficiently large to warrant further investigation as to their effect upon larger circulations.

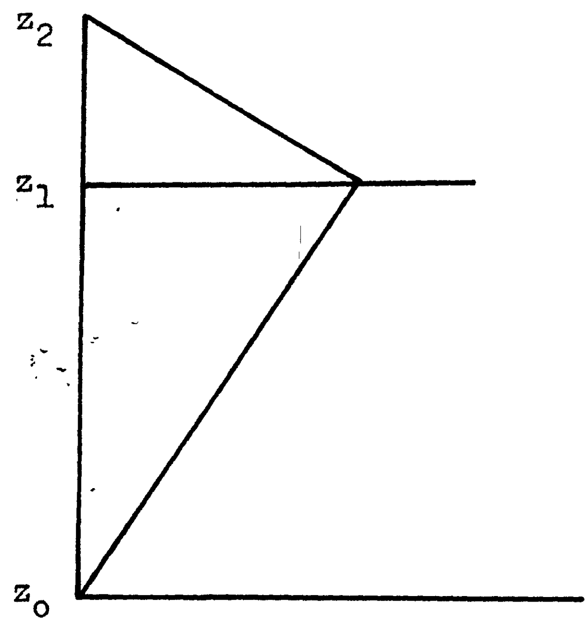

Linear Updraft Profile

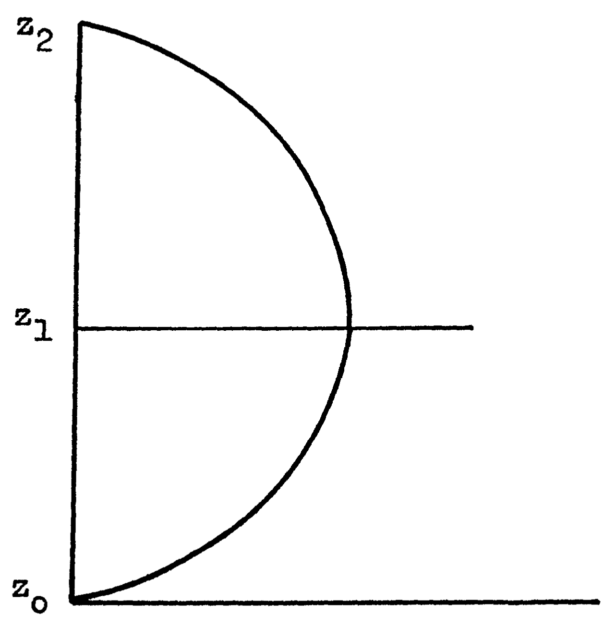

Parabolic Updraft Profile

Figure 1. Updraft Velocity Profiles
Maximum vertical velocity at level z_1.

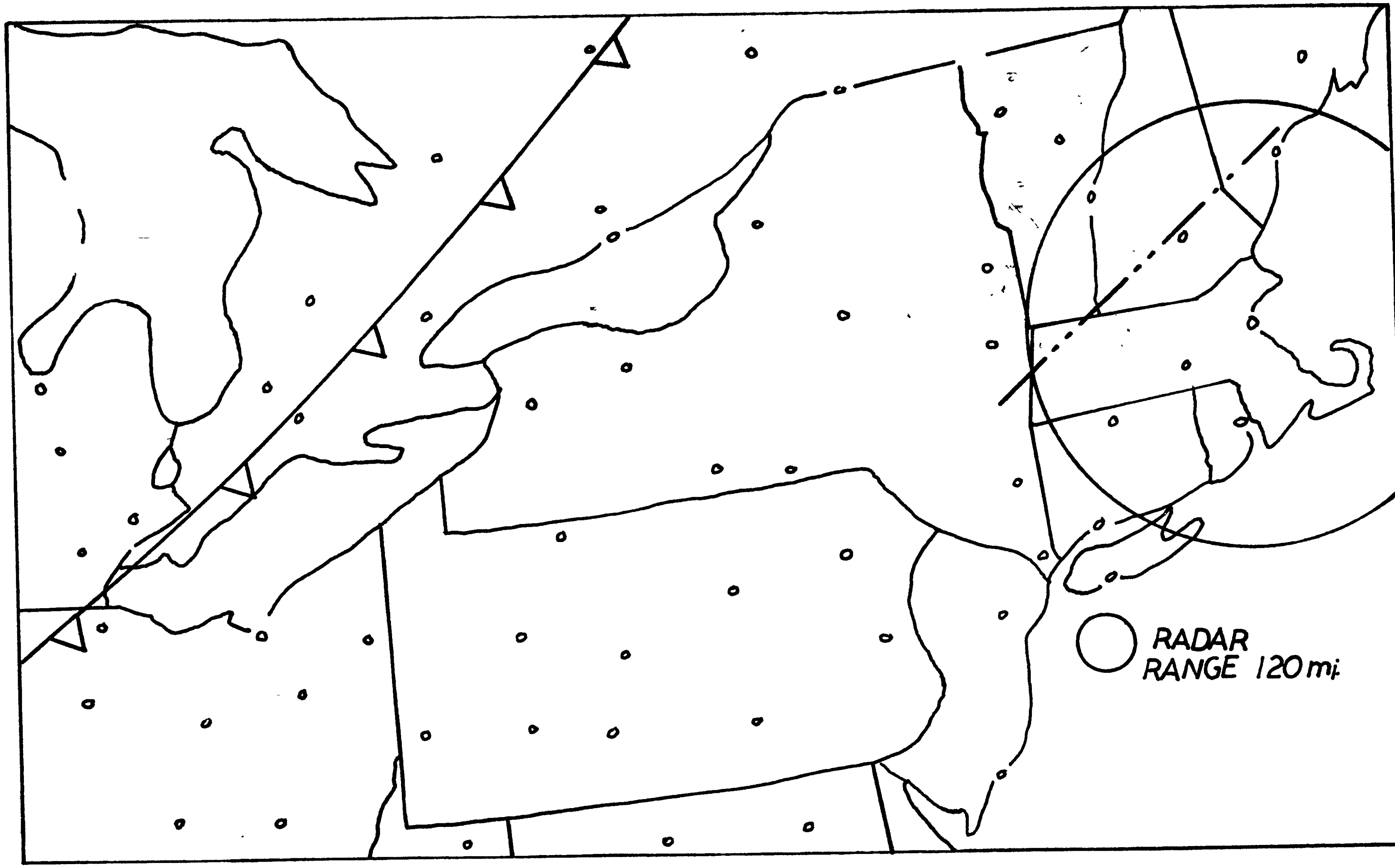

FIGURE 2. SURFACE FEATURES AT 0900EST ON JUNE 9, 1965

FIGURE 3. SURFACE FEATURES AT 1800EST ON JUNE 9, 1965

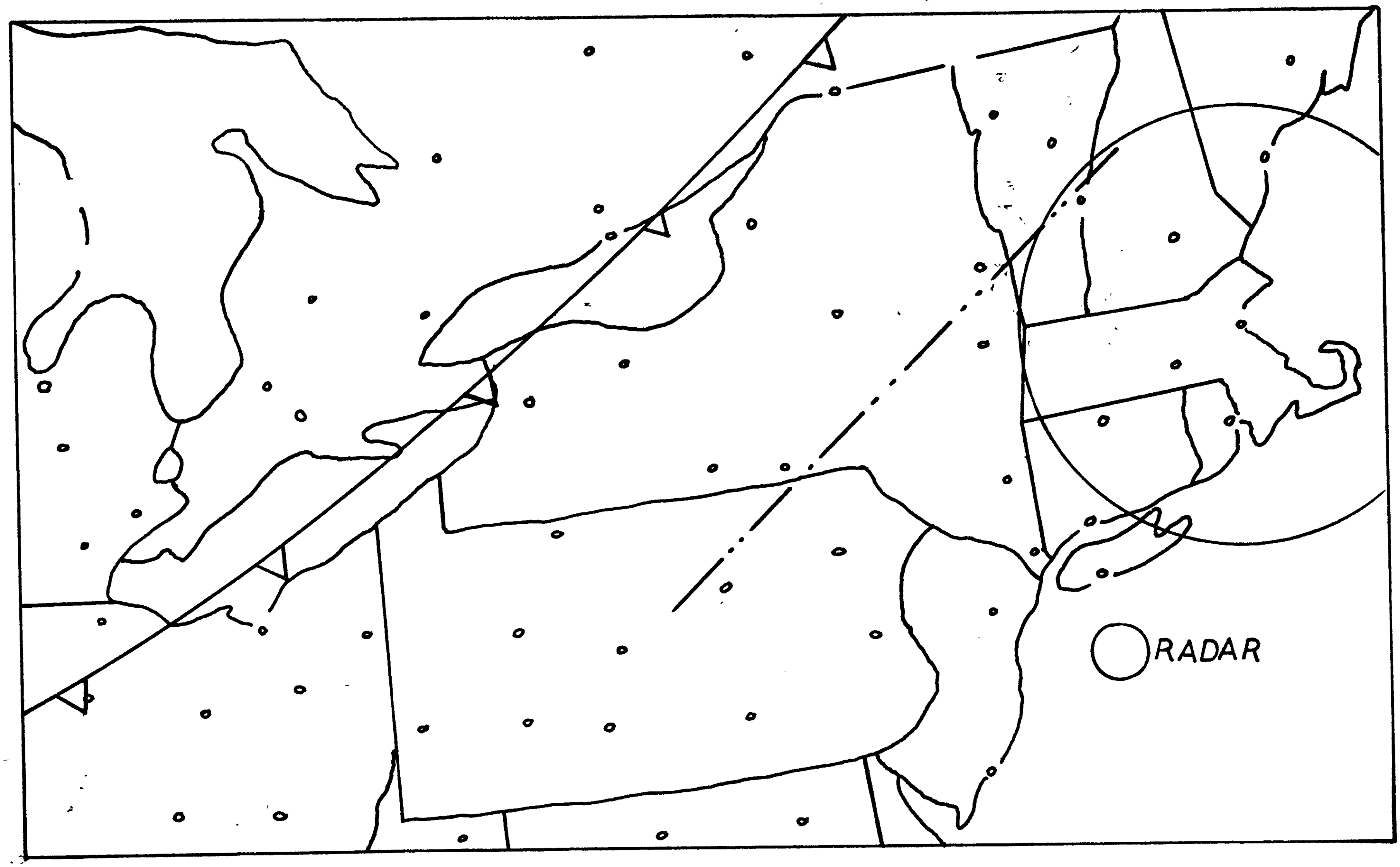

FIGURE 4. SURFACE FEATURES AT 1800EST ON JUNE 23, 1965

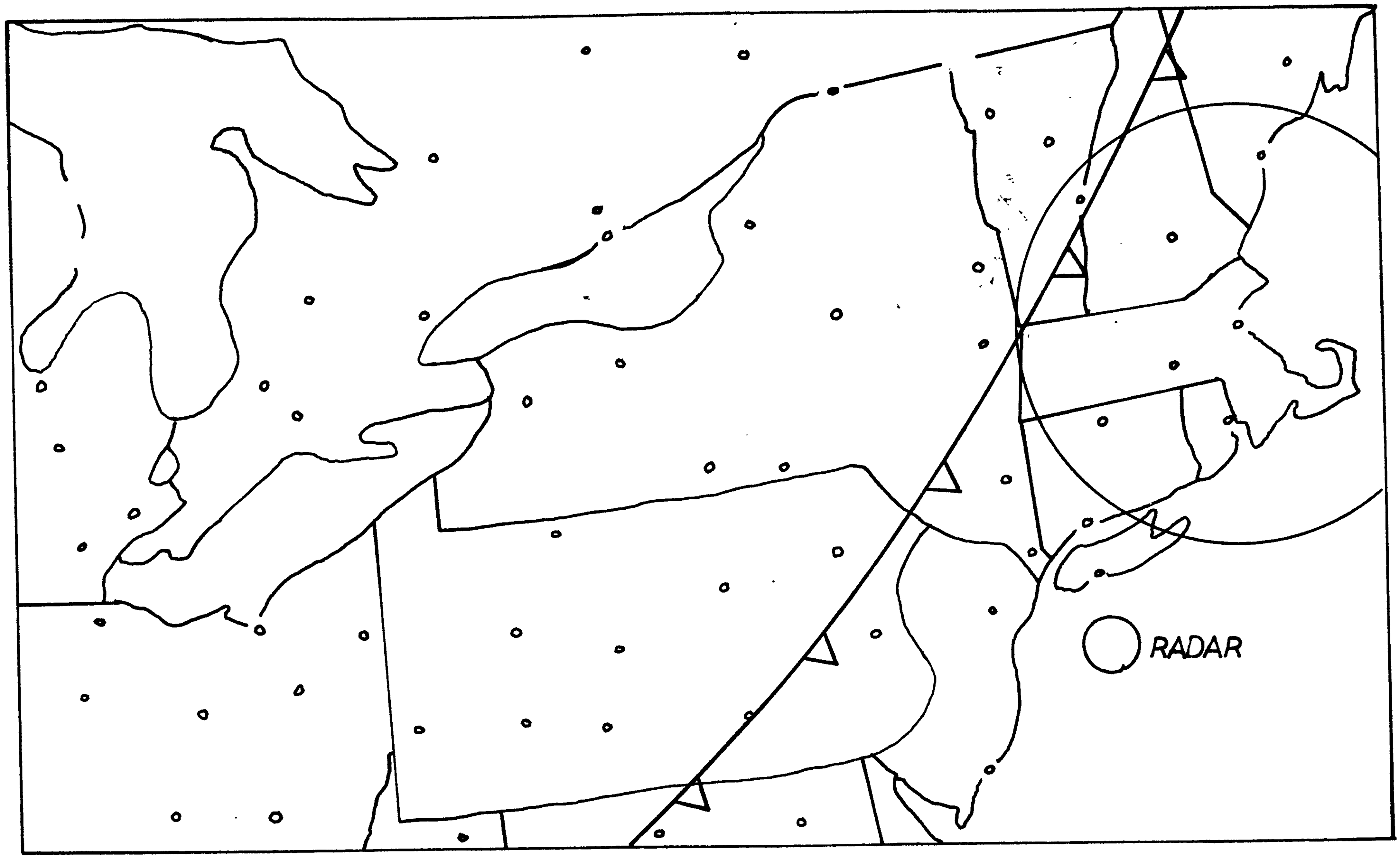

FIGURE 5. SURFACE FEATURES AT 0900EST ON JUNE 24, 1965

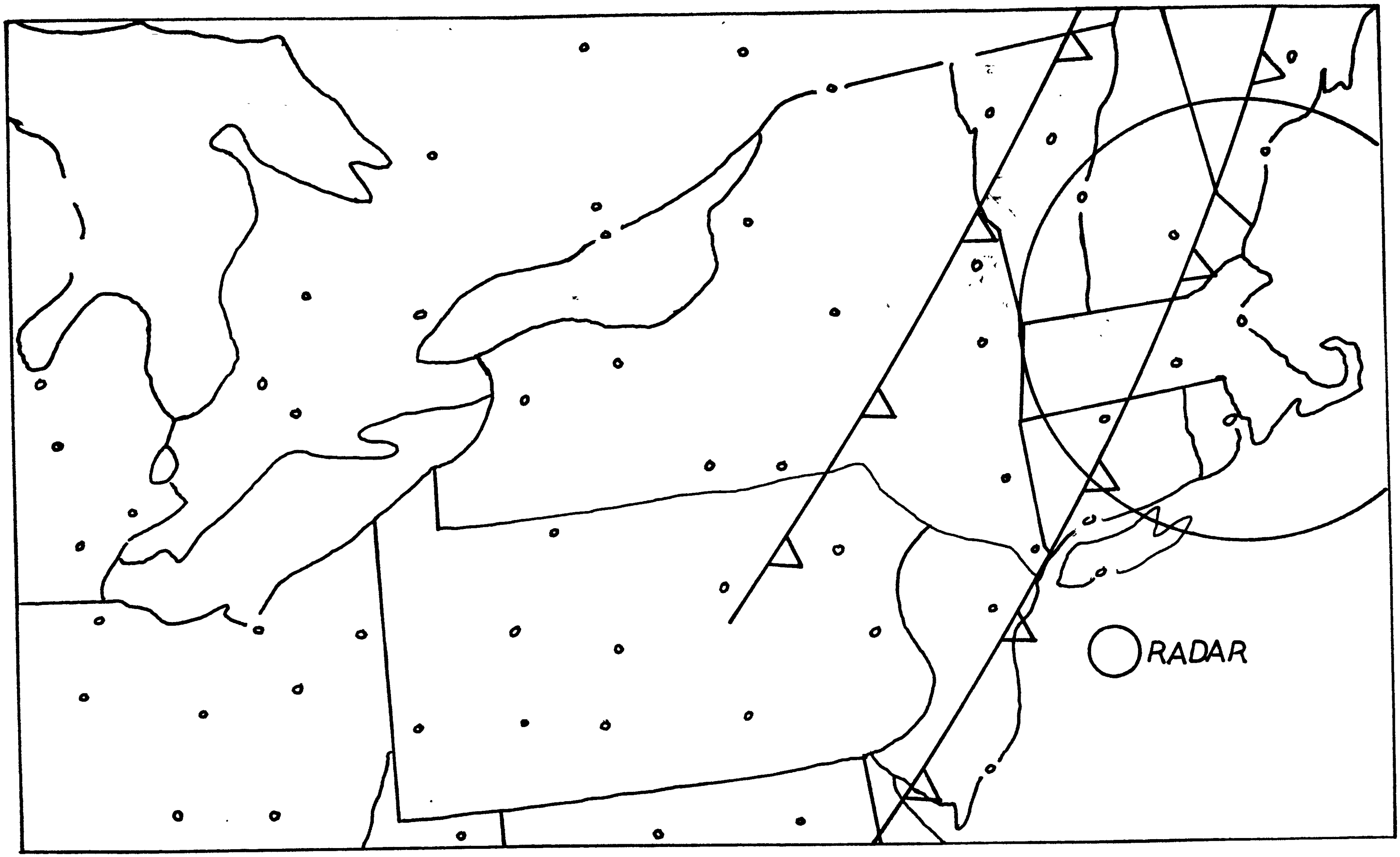

FIGURE 6. SURFACE FEATURES AT 1400EST ON AUGUST 28, 1965

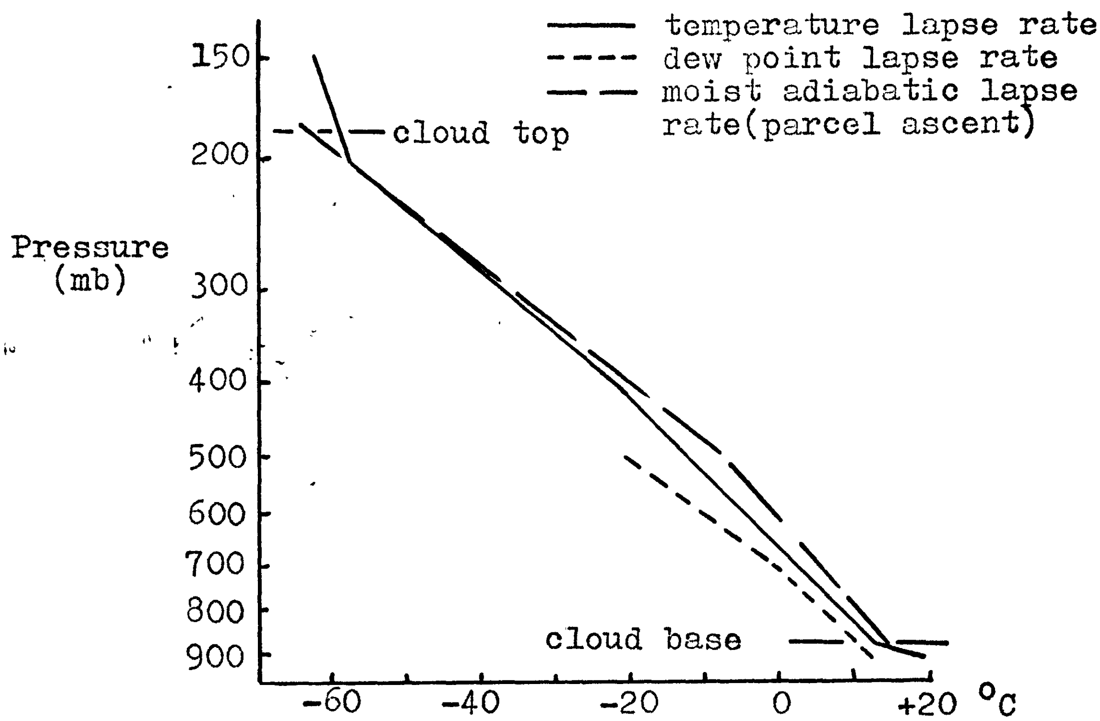

Figure 7. Sounding for Albany, N.Y., at 0700EST, June 9, 1965.

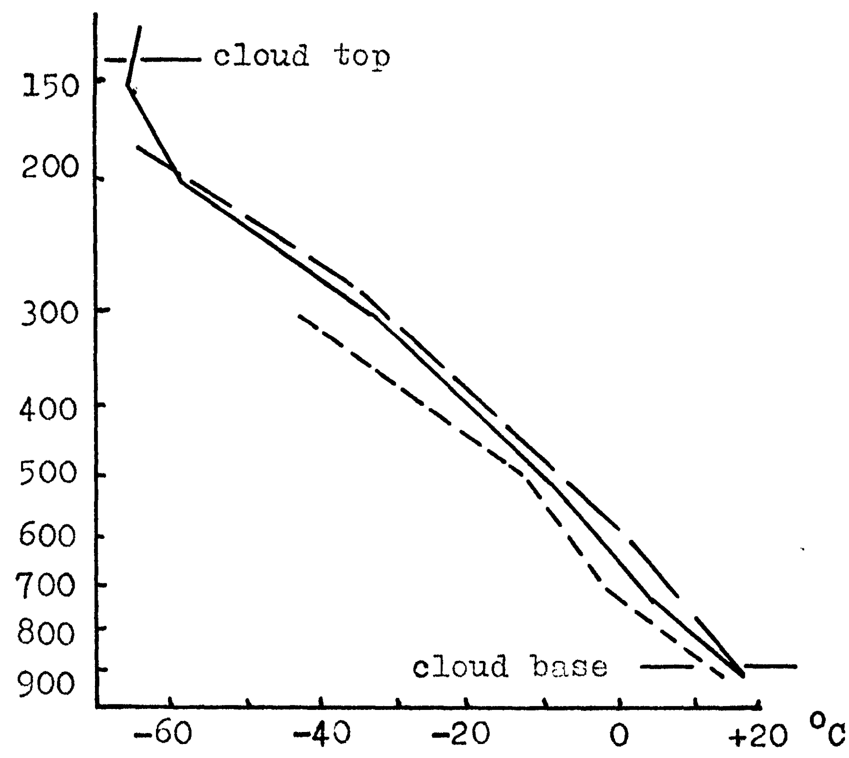

Figure 8. Sounding for Albany, N.Y., at 1900EST, June 23, 1965.

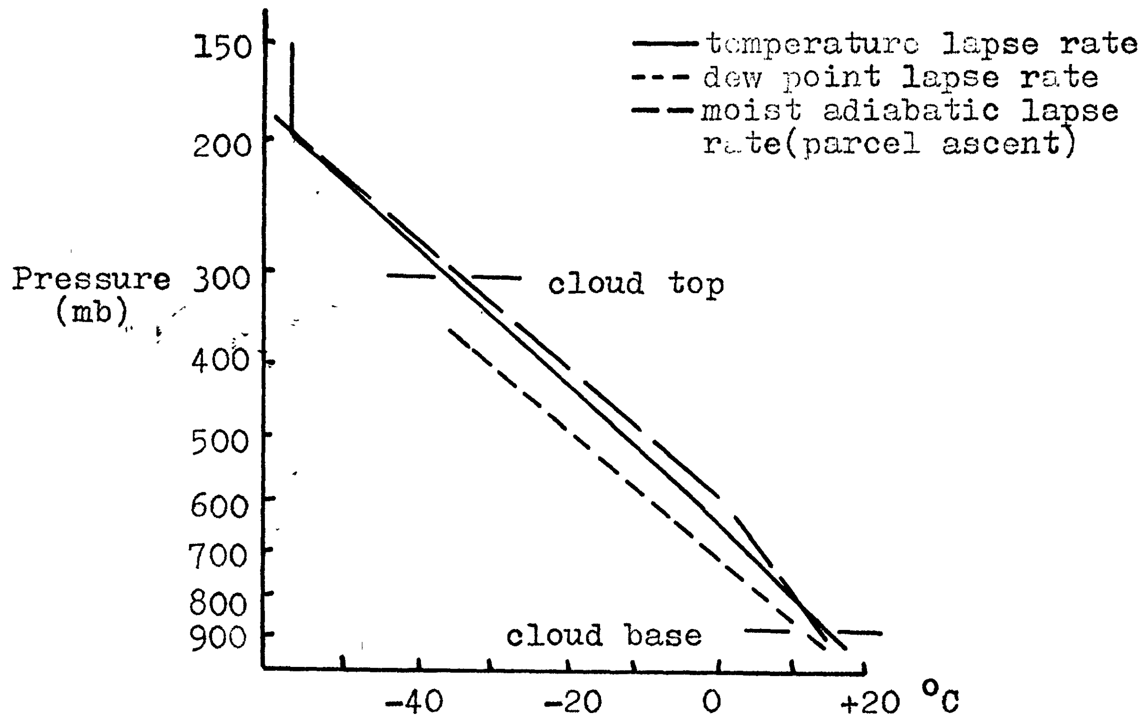

Figure 9. Sounding for Portland, Me. 0700EST, June 24, 1965.

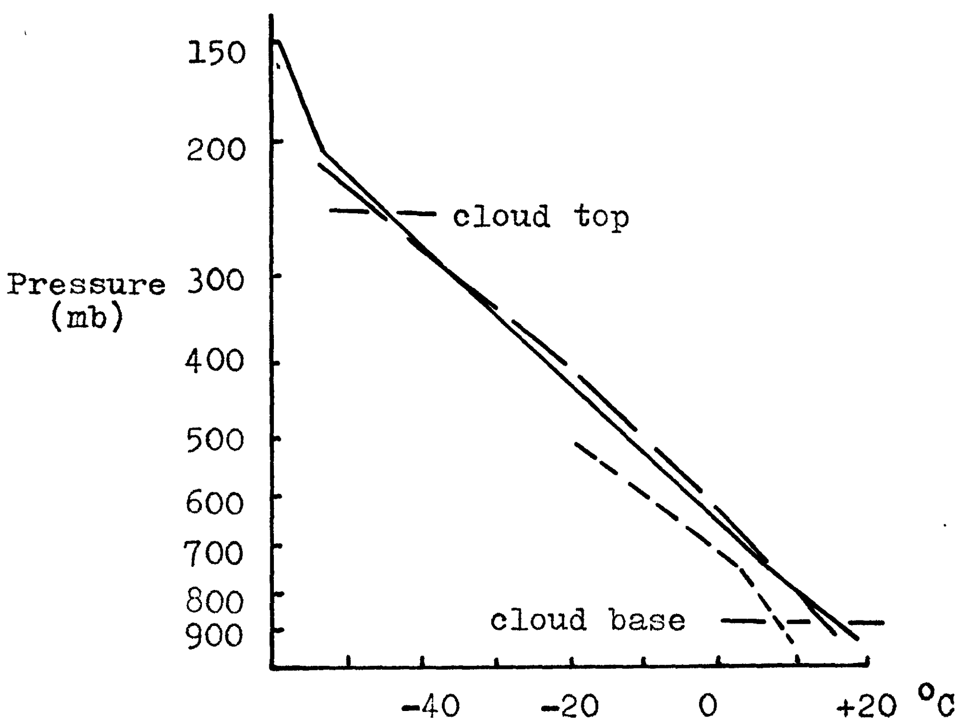

Figure 10. Sounding from average conditions at Portland, Me., Albany, N.Y., and Nantucket, Mass., 1300EST, August 28, 1965.

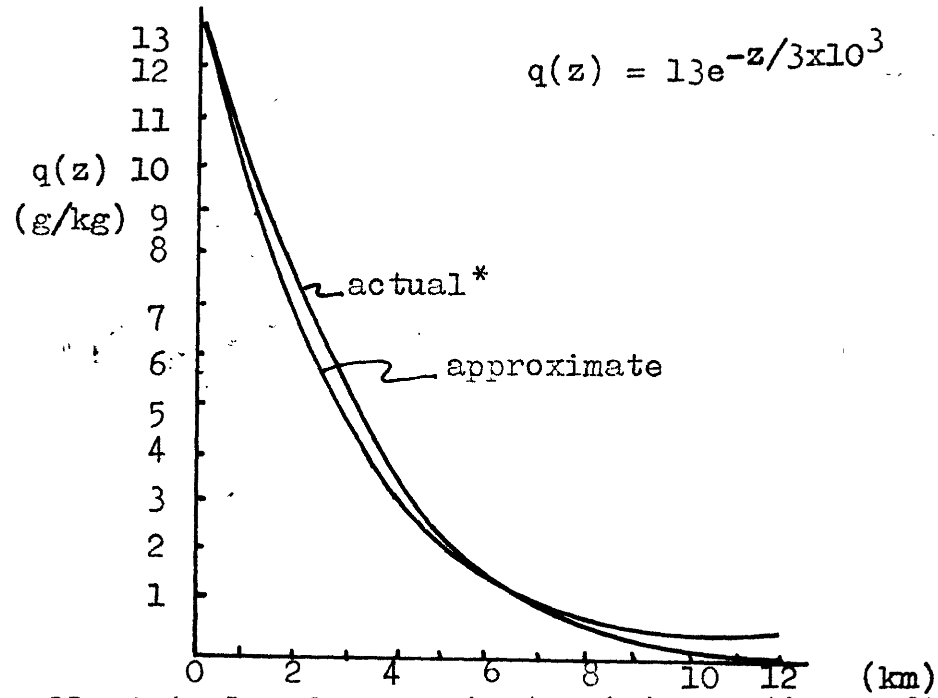

Figure 11. Actual and approximate mixing ratio profiles for 0700 EST, June 9, 1965, Albany, N.Y.

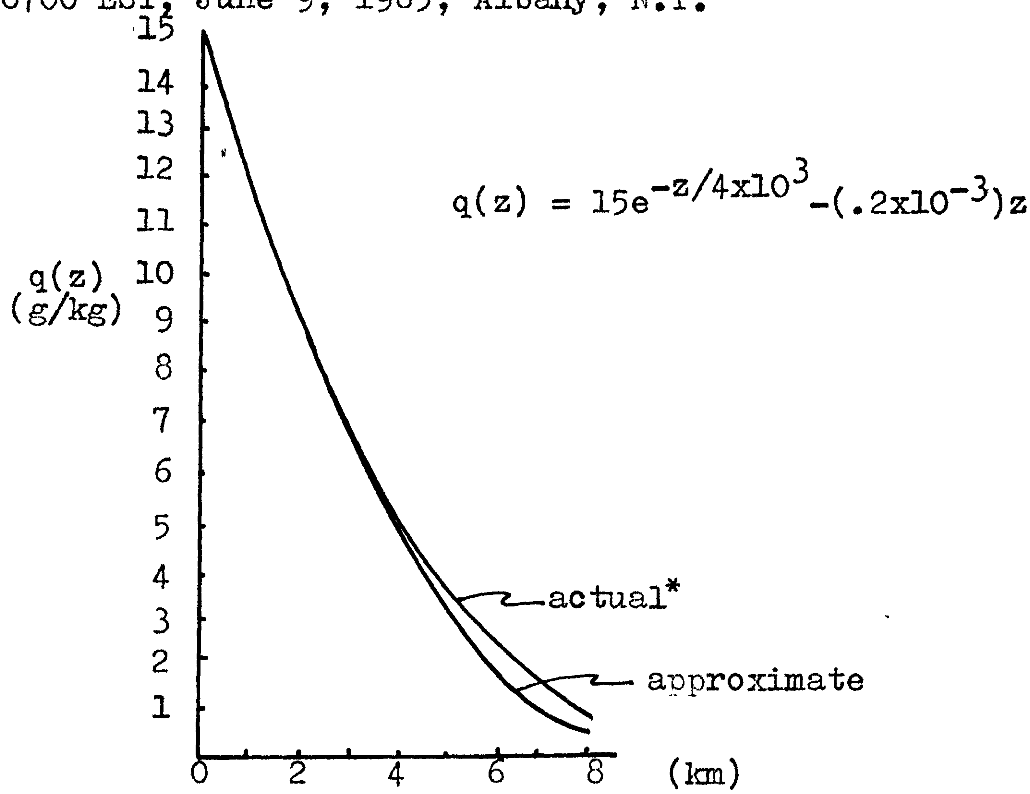

Figure 12. Actual and approximate mixing ratio profiles for 0700 EST, June 24, 1965, Portland, Me.

*Actual refers to saturated conditions within complex.

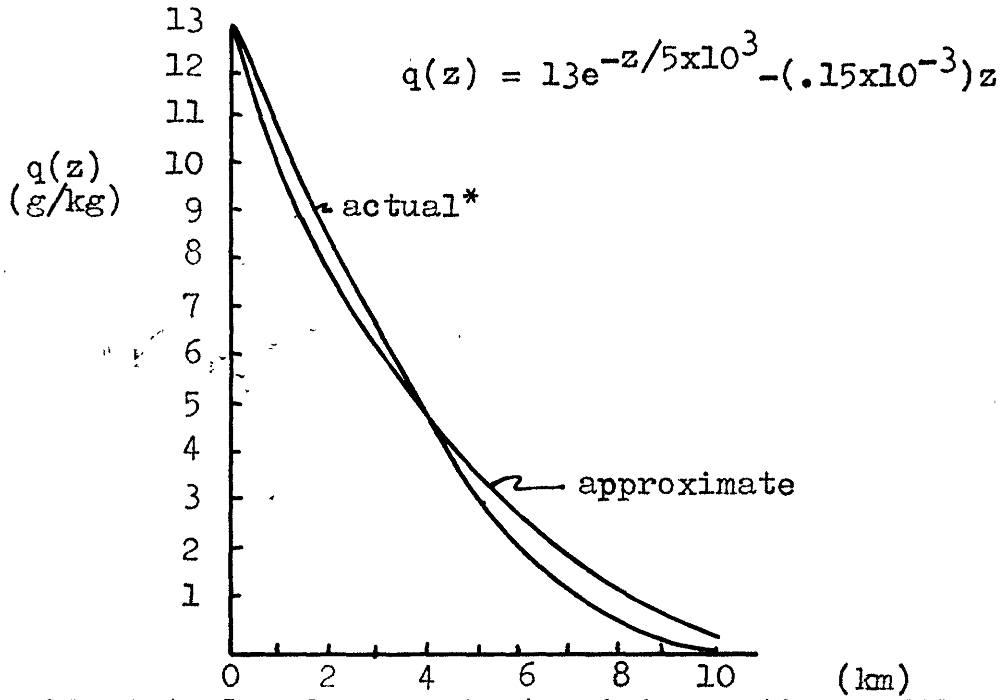

Figure 13. Actual and approximate mixing ratio profiles for average conditions, 1300EST, August 28, 1965, ALB, ACK, PWM.

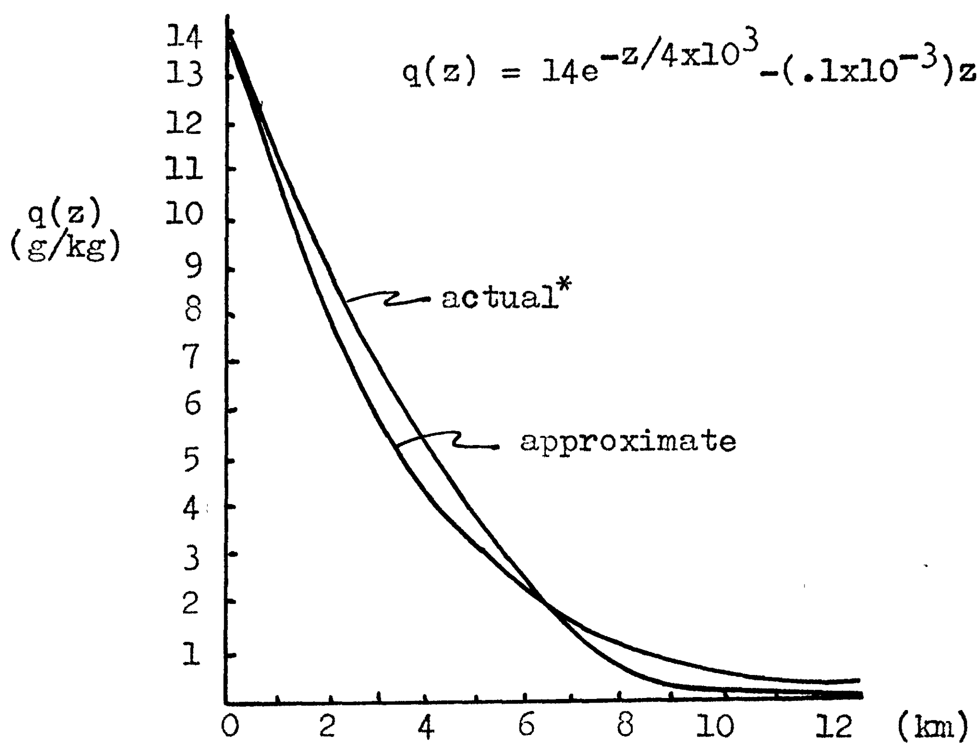

Figure 14. Actual and approximate mixing ratio profiles for 1900EST, June 23, 1965, Albany, N.Y.
*Actual refers to saturated conditions within complex.

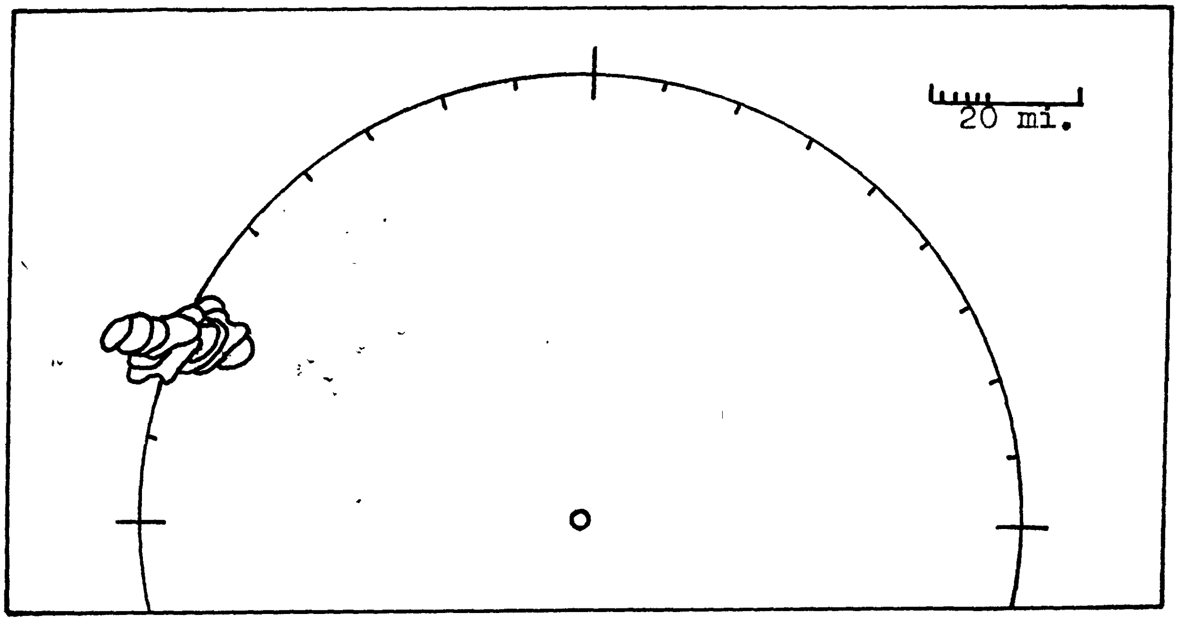

Figure 15. Motion and development of the complex in Case I from 0915EST to 1013EST on June 9, 1965.

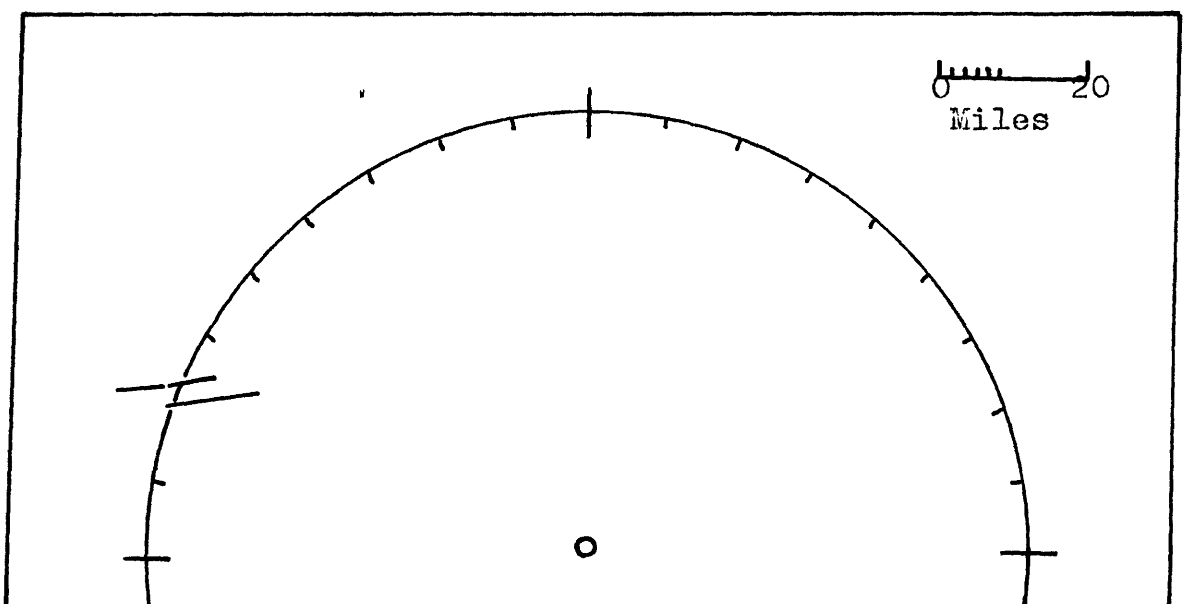

Figure 16. Motion of the cells in Case I on June 9, 1965.

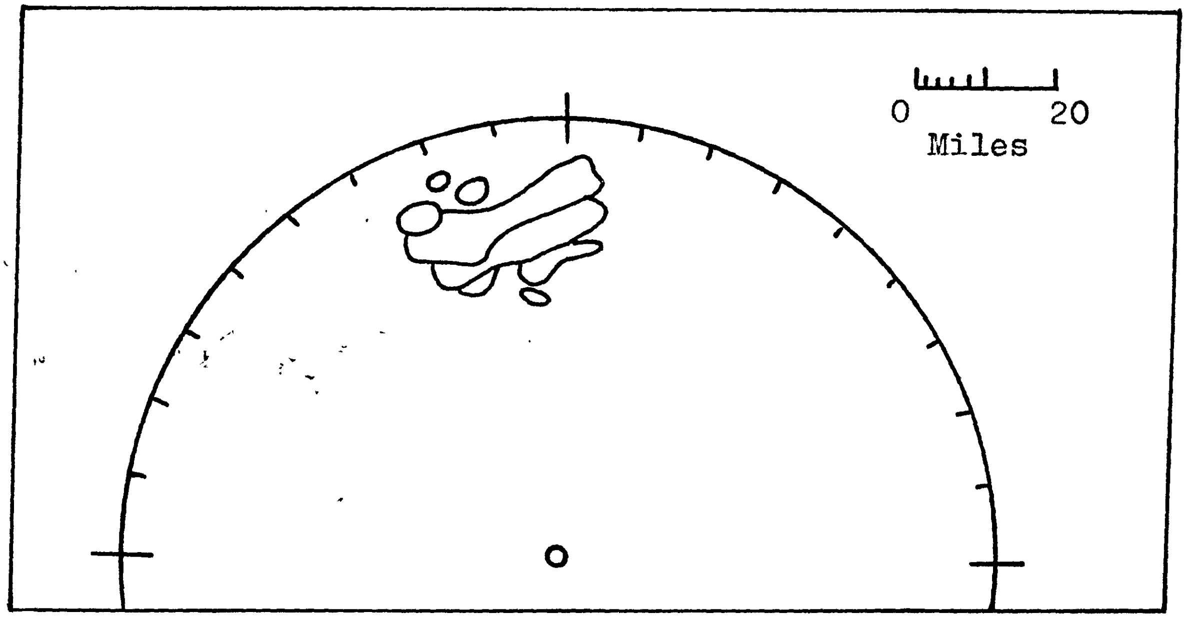

Figure 17. Motion and development of the complex in Case II from 1837EST to 2106EST on June 9, 1965.

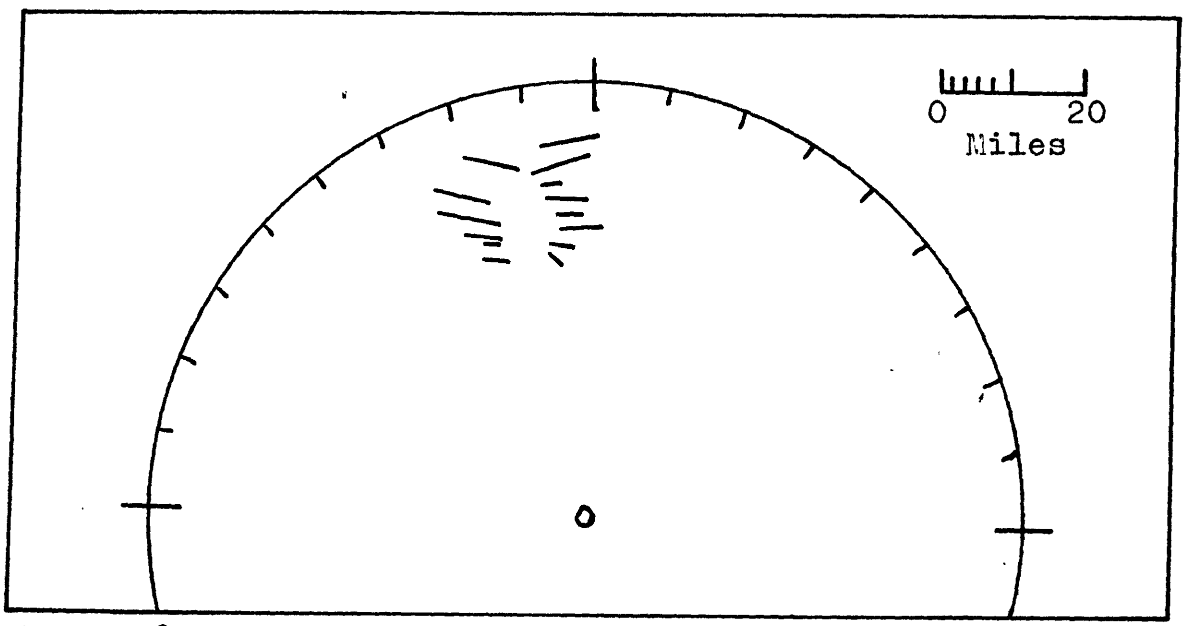

Figure 18. Motion of the cells in Case II on June 9, 1965.

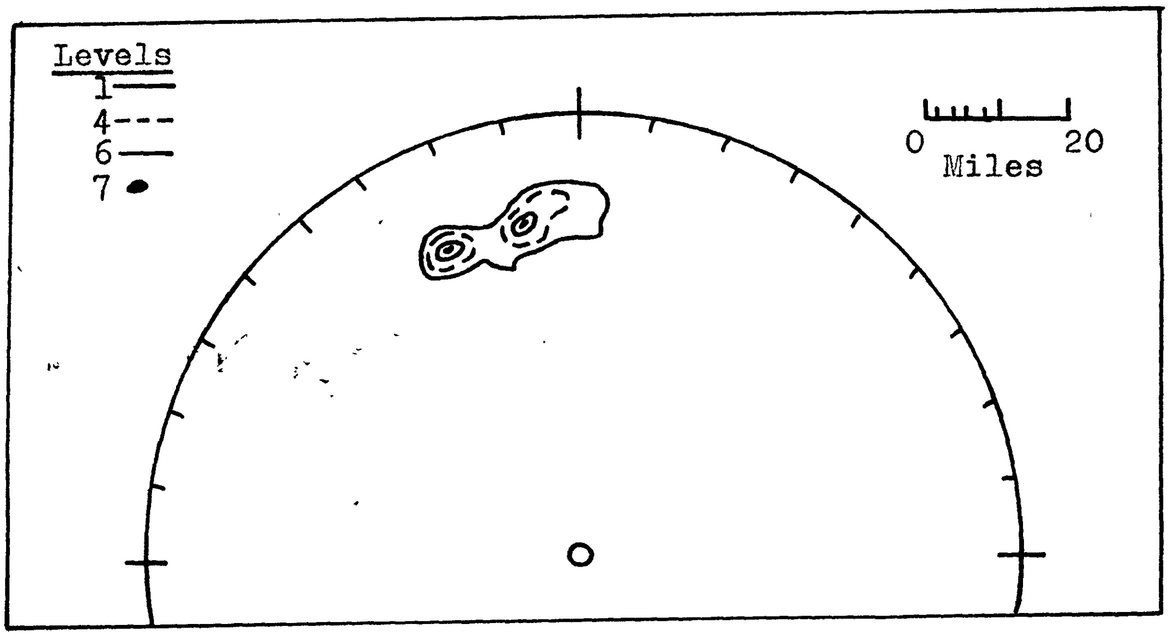

Figure 19. PPI of storm complex in Case II at 1953EST on June 9, 1965.

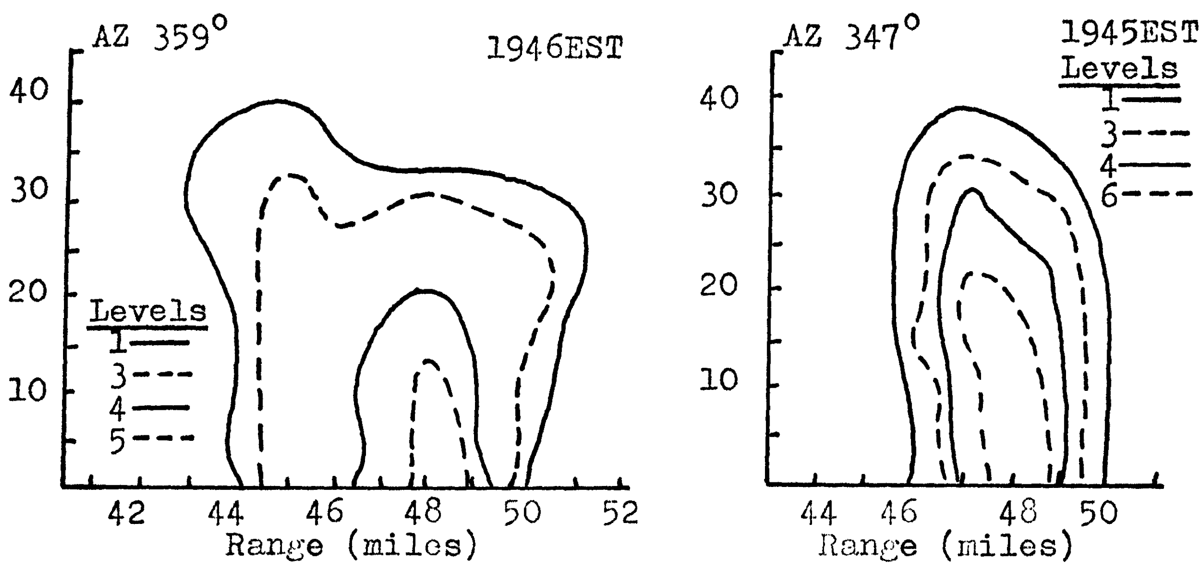

Figure 20. RHI display of vertical sections through the complex in Case II which is shown in Figure 19. Altitudes are given in thousands of feet.

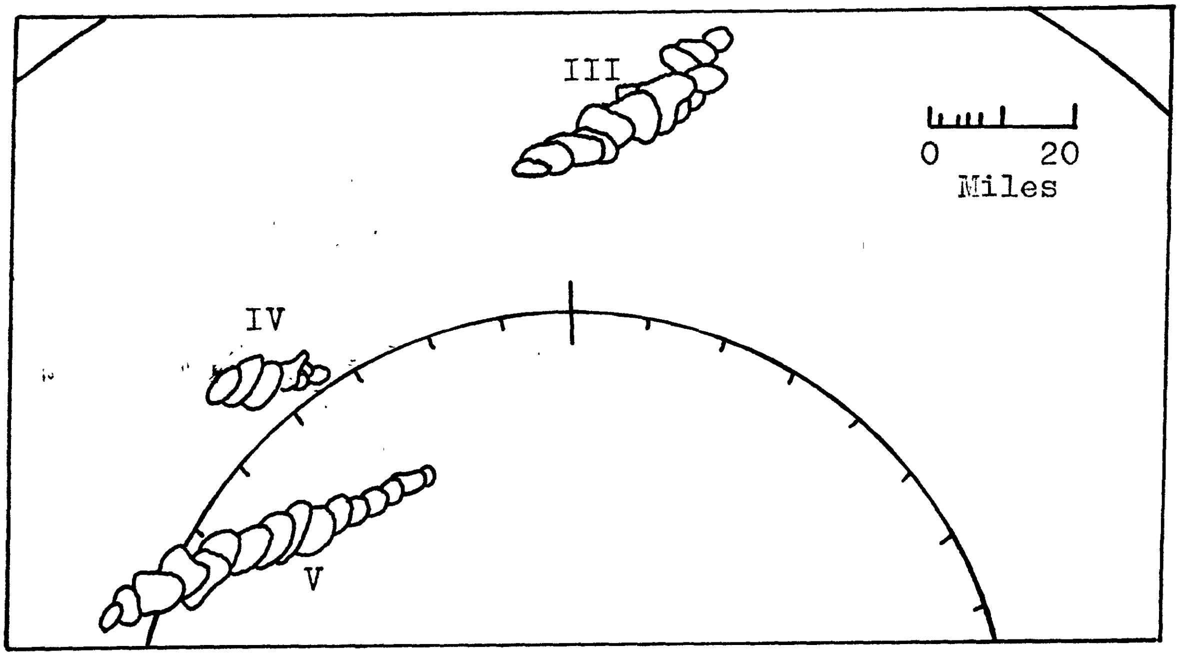

Figure 21. Motion and development of the complexes in Cases III, IV, and V, on June 23, 1965.

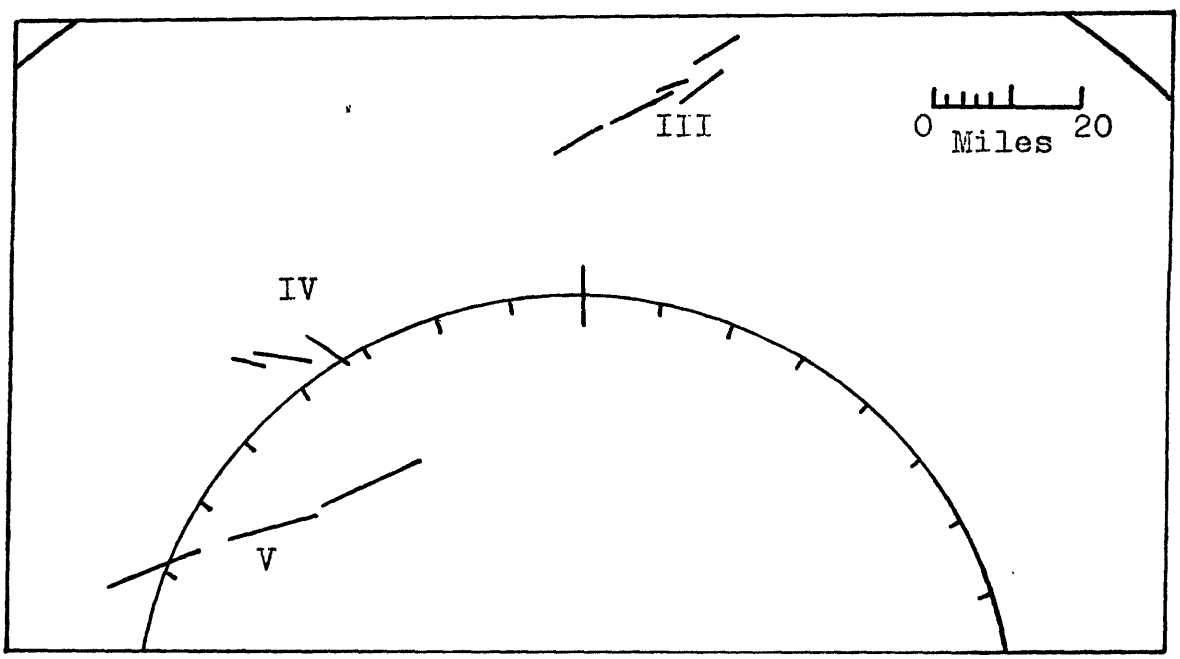

Figure 22. Motion of the cells in Cases III, IV, and V on June 23, 1965.

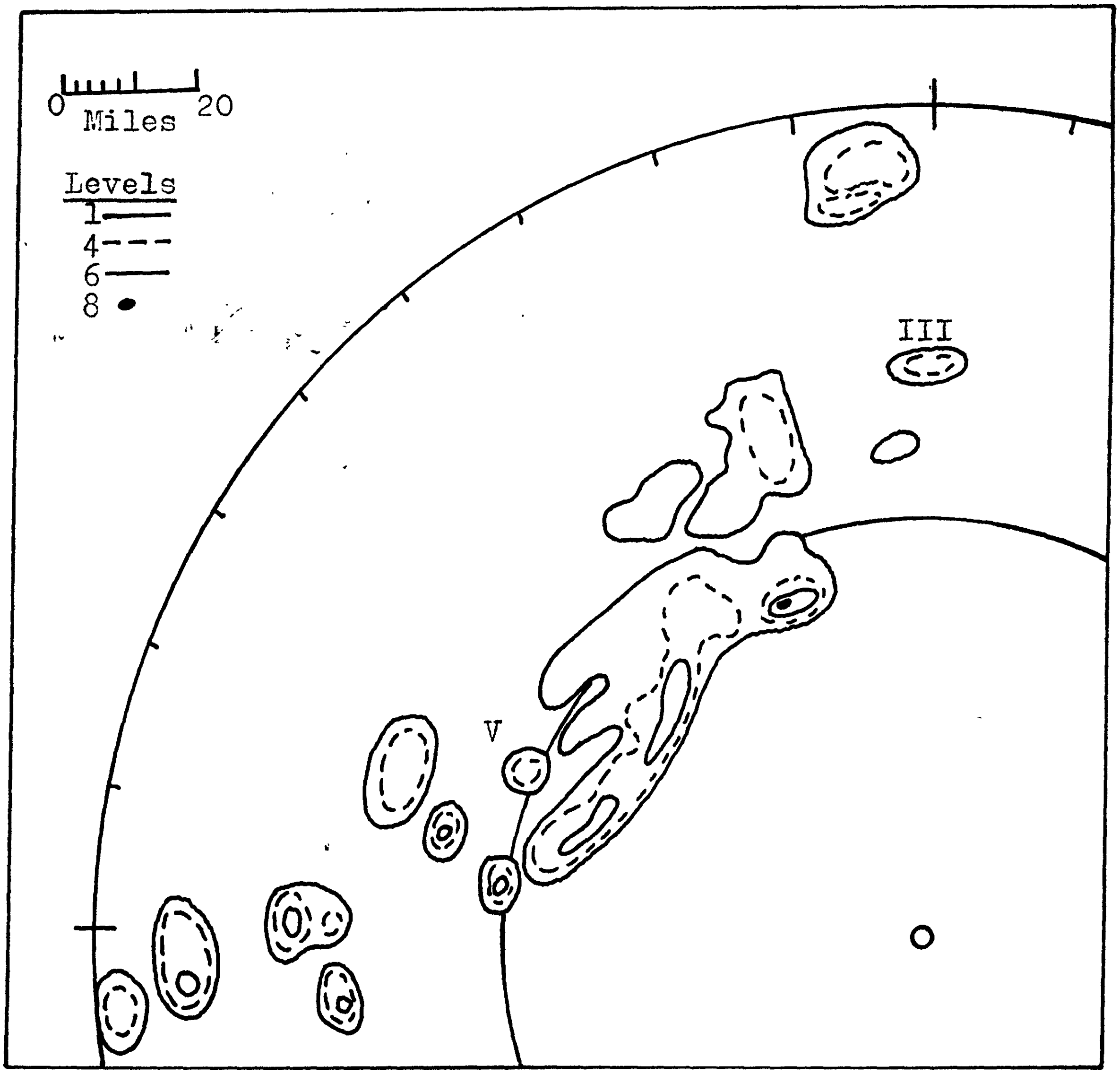

Figure 23. PPI at 1816EST, June 23, 1965, of the squall line in which storm Cases III, IV, and V occurred. The complexes in Cases III and V are in existence at this time.

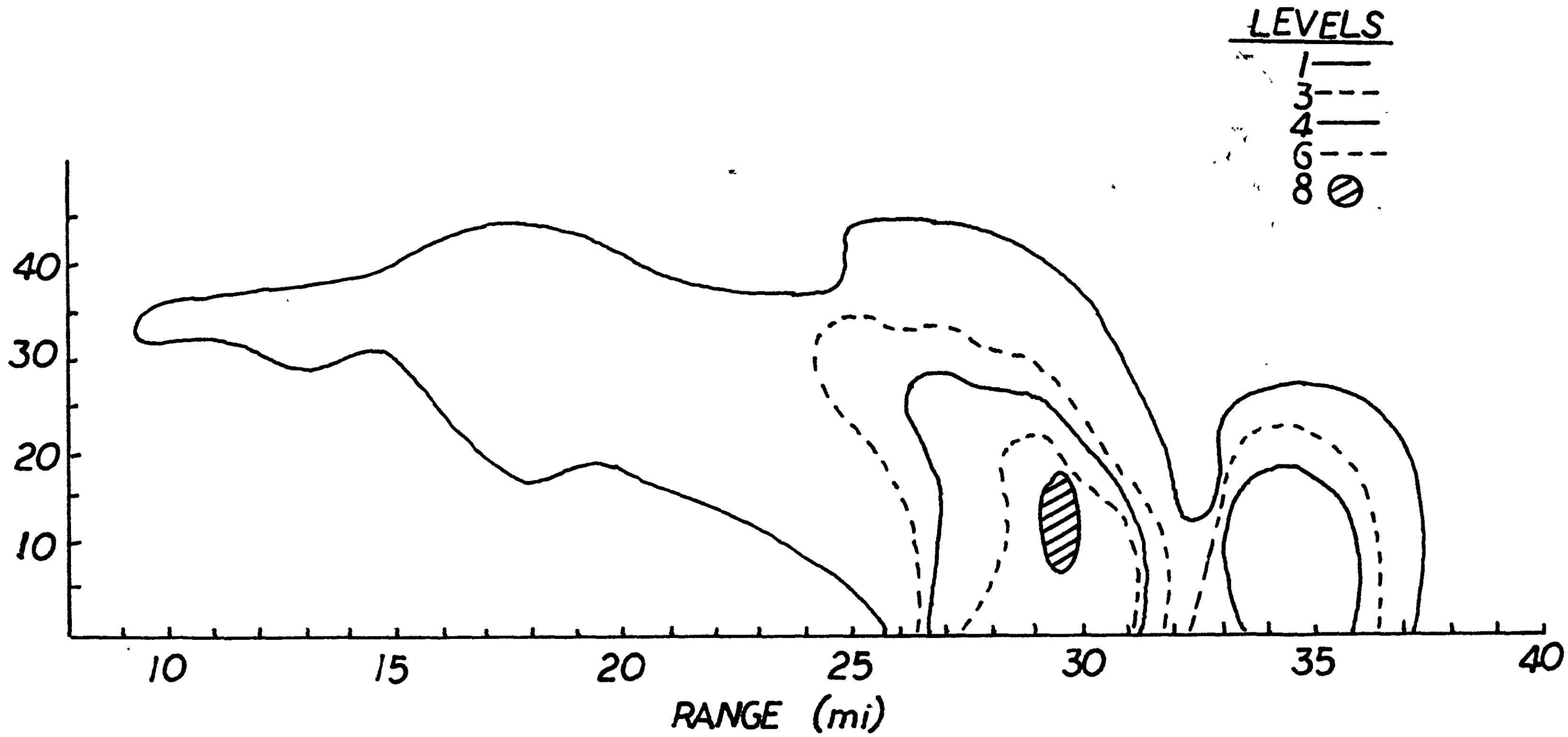

FIGURE 24. RHI DISPLAY OF A VERTICAL SECTION THROUGH THE SQUALL LINE IN FIGURE 23 AT 1937EST AND AZIMUTH 301.° ALTITUDE IN THOUSAND FEET.

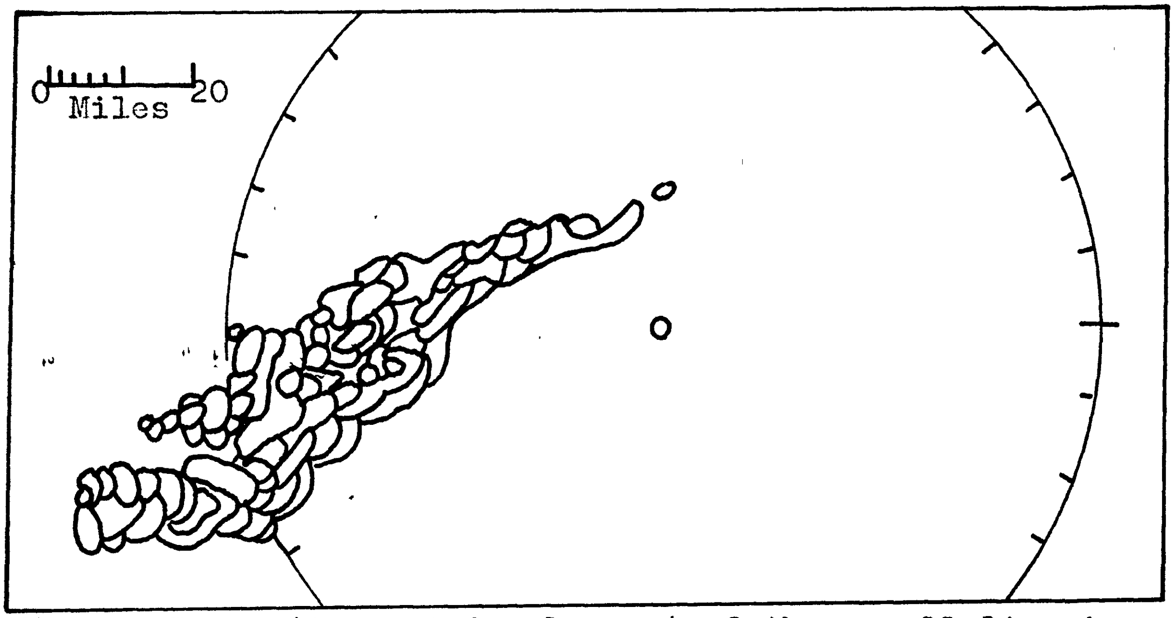

Figure 25. Motion and development of the squall line in Case VI from 0958EST until 1100EST on June 24, 1965.

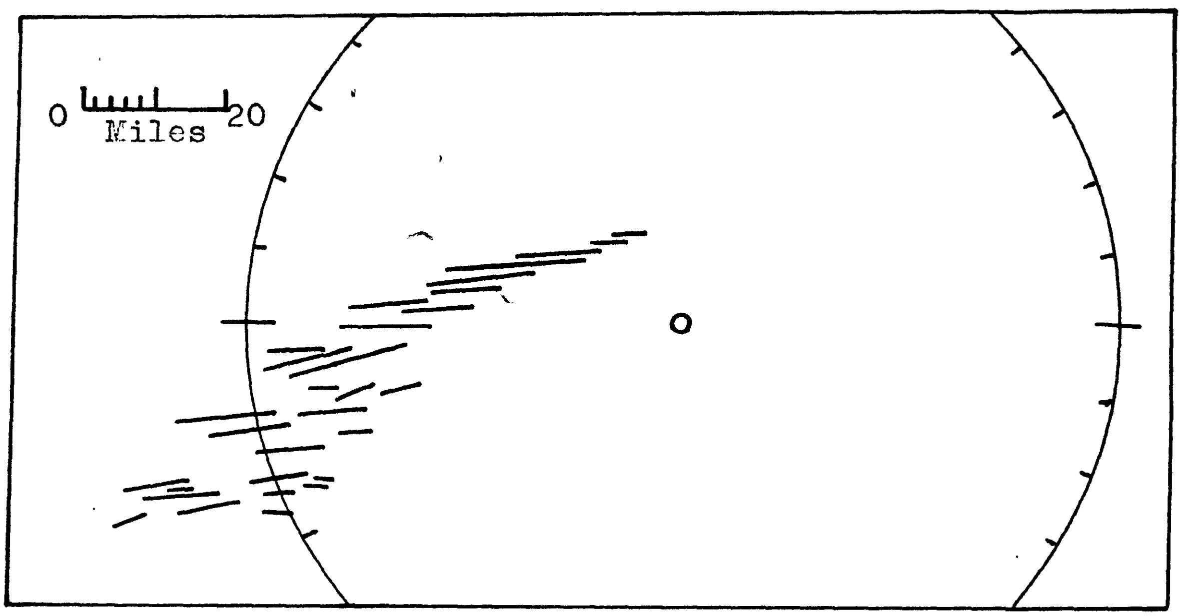

Figure 26. Motion of the cells in Case VI, June 24, 1965.

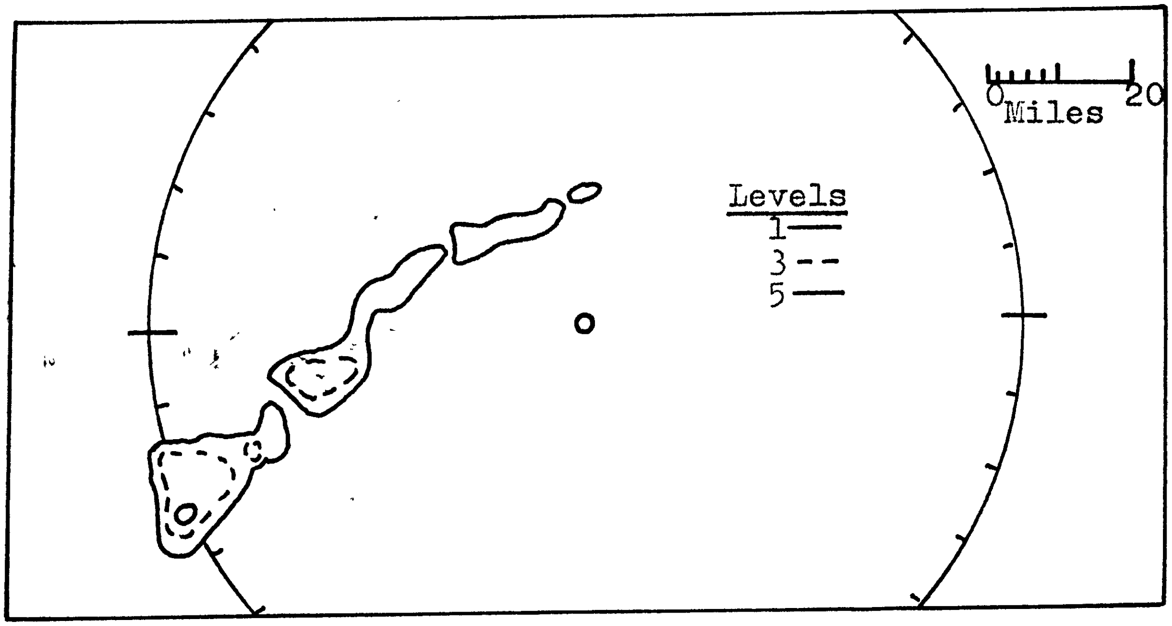

Figure 27. PPI at 1101EST, June 24, 1965, of the squall line in Case VI.

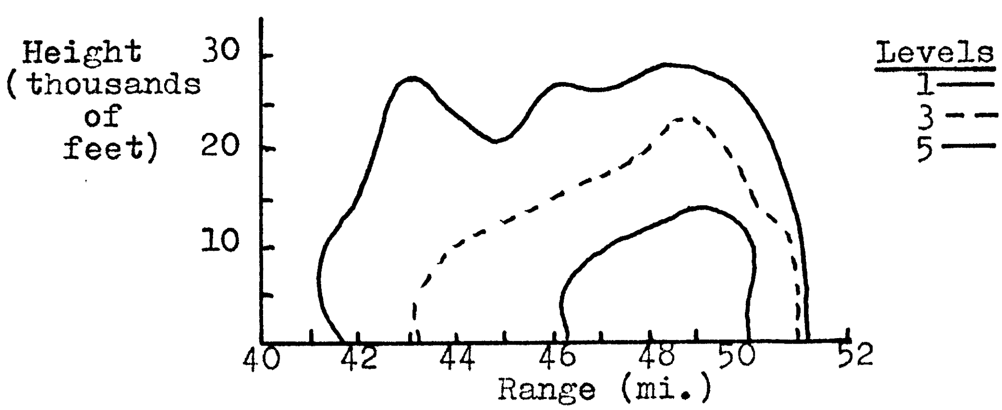

Figure 28. RHI display of a vertical section through the squall line in Case VI at 1130EST and azimuth 240°.

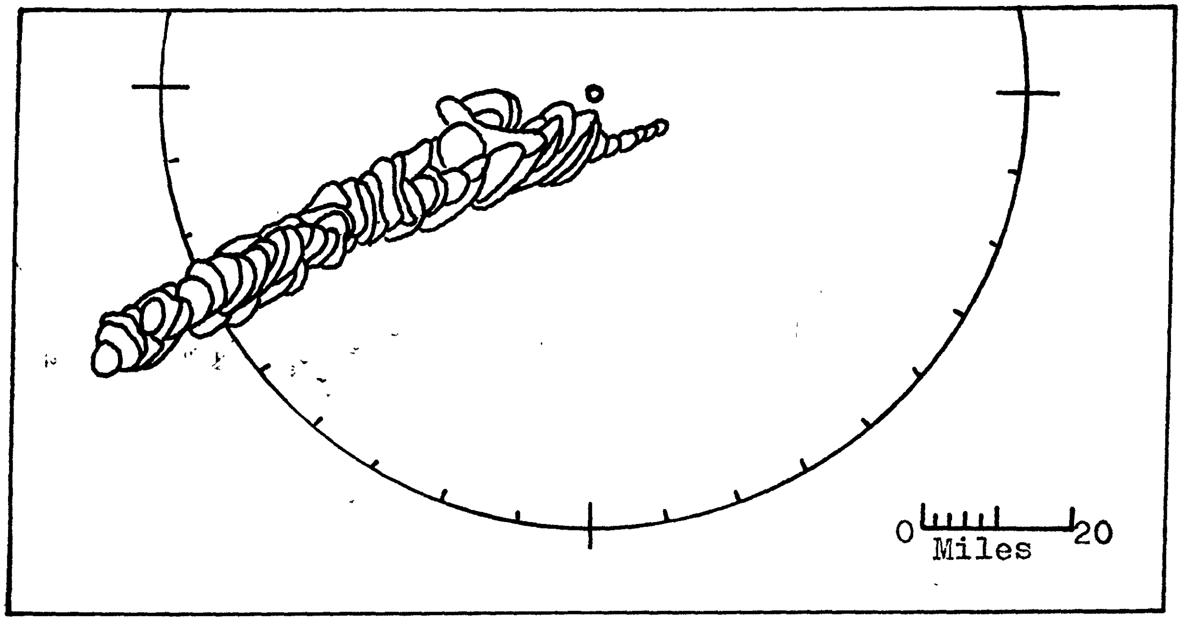

Figure 29. Motion and development of the complex in Case VII from 1454EST to 1652EST, August 28, 1965.

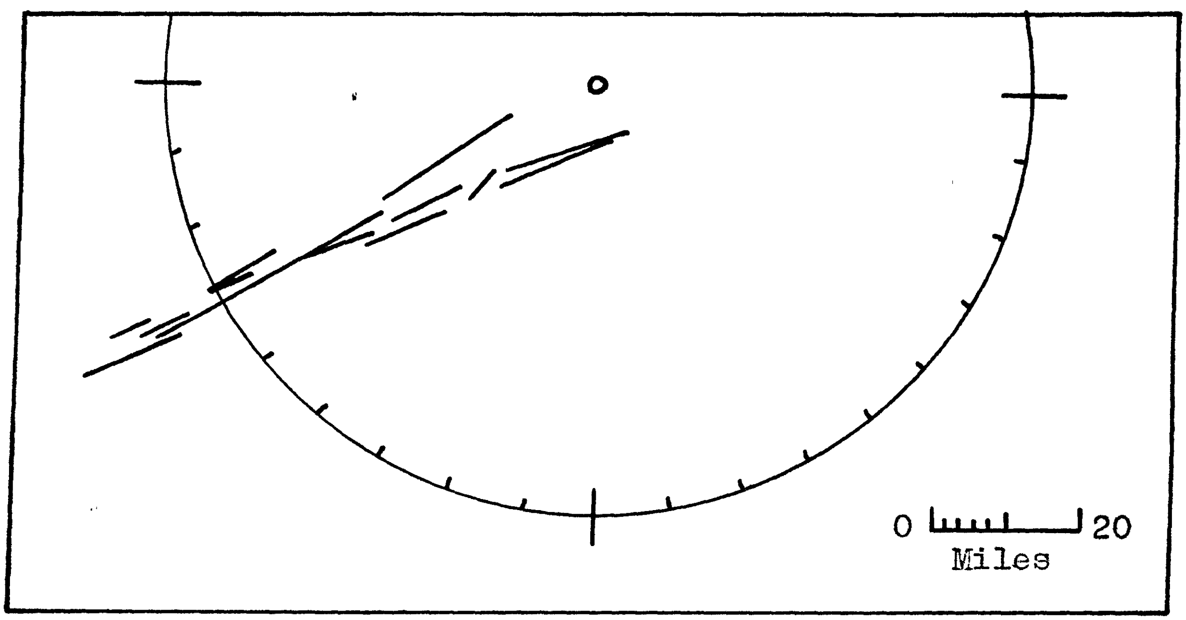

Figure 30. Cell movement in Case VII, August 28, 1965.

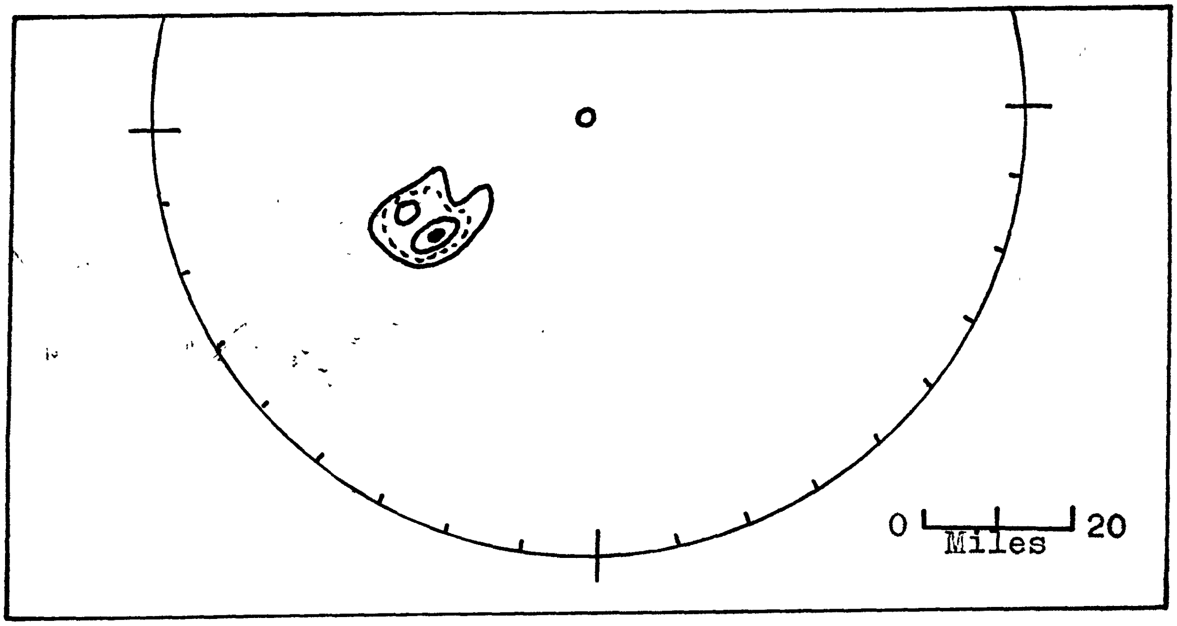

Figure 31. PPI at 1609EST, August 28, 1965, of the complex in Case VII.

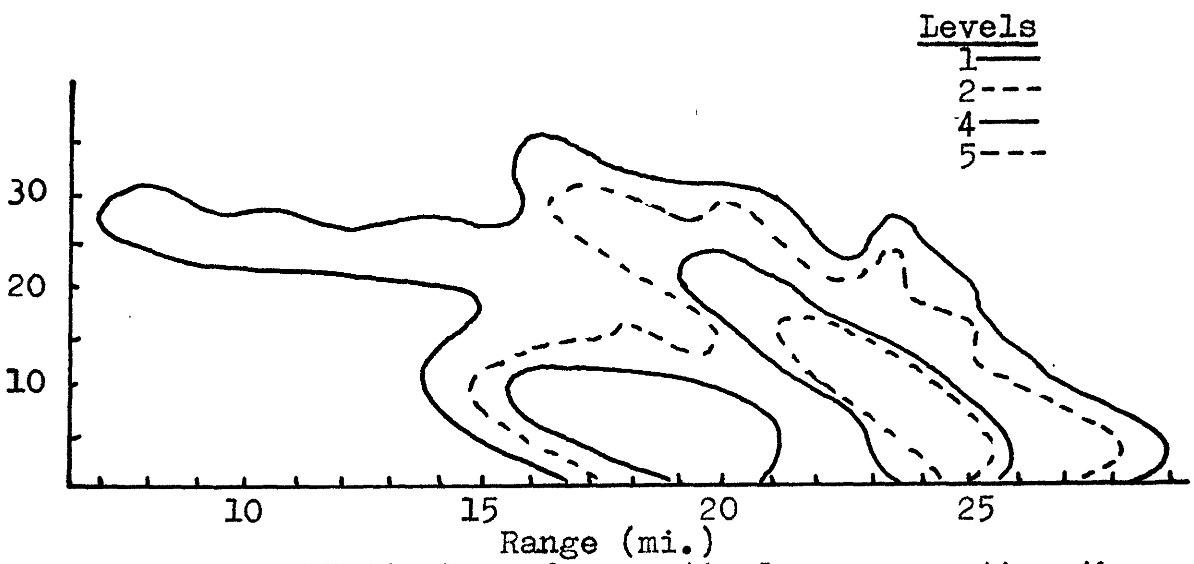

Figure 32. RHI display of a vertical cross section through the complex in Case VII at 1612 EST and azimuth 235°.

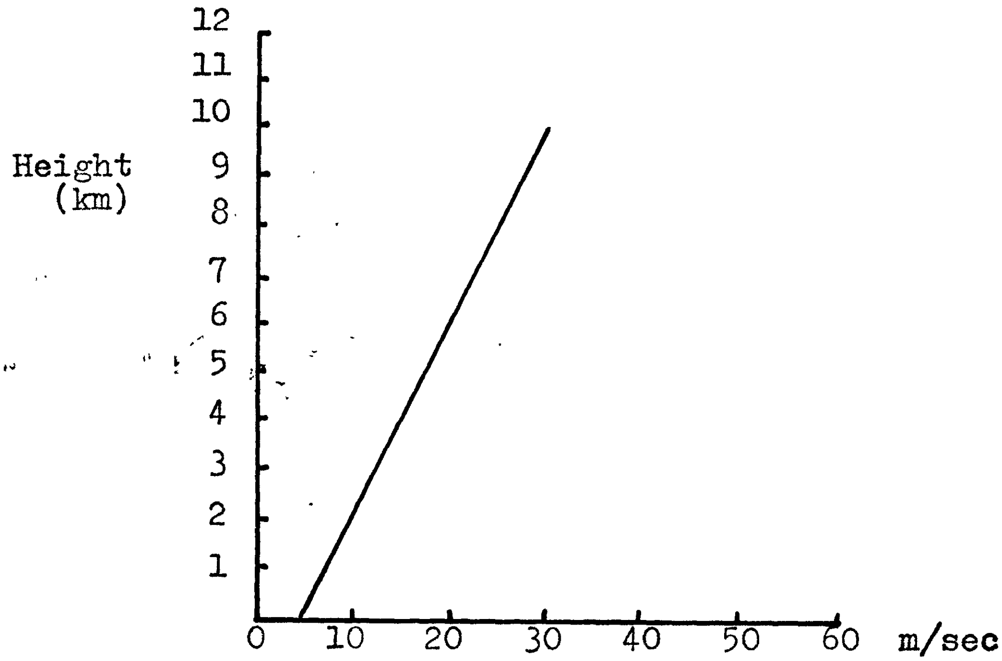

Figure 33. Wind profile at 0700EST, June 9, 1965.

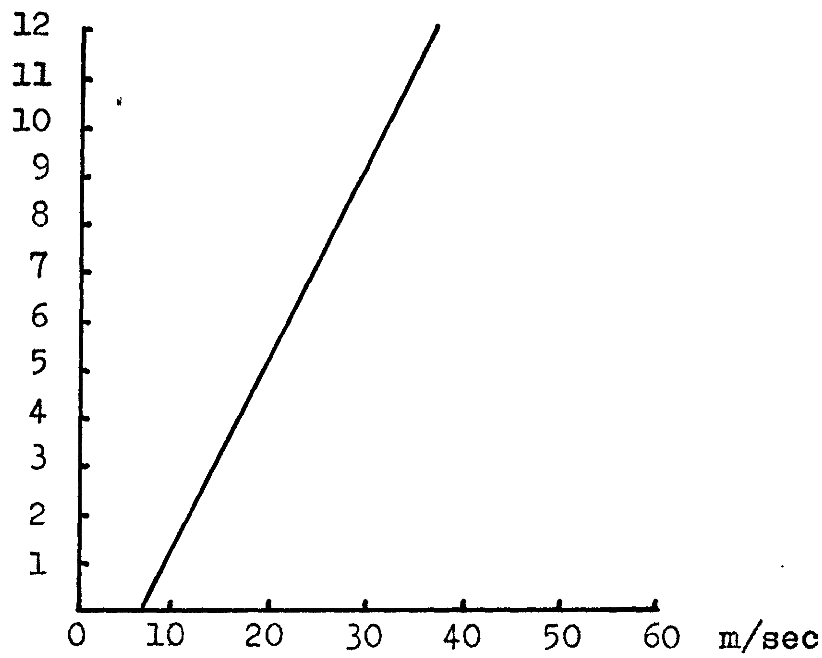

Figure 34. Wind profile at 1900EST, June 9, 1965.

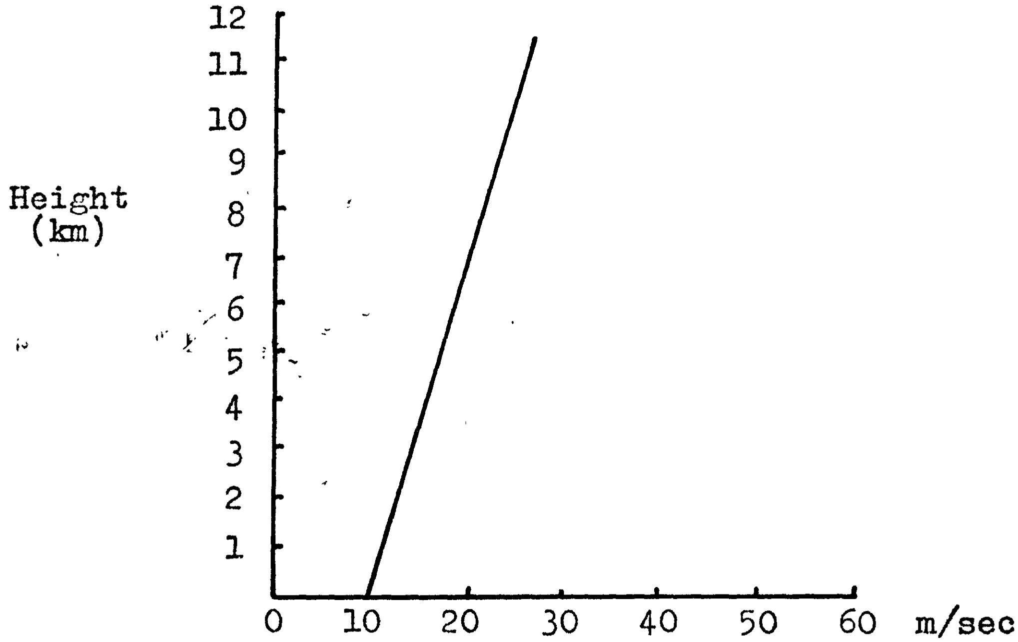

Figure 35. Wind profile at 1900EST, June 23, 1965.

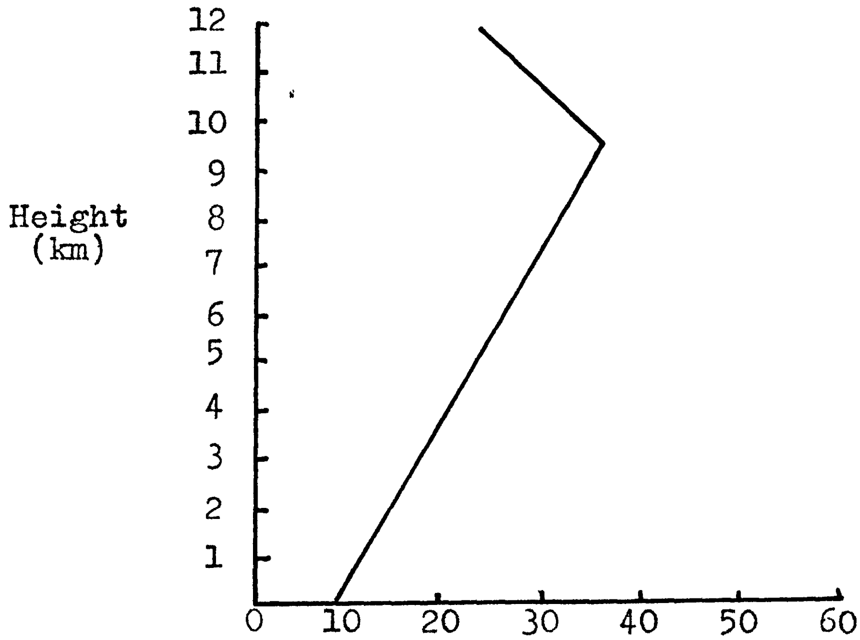

Figure 36. Wind profile at 0700EST, June 24, 1965.

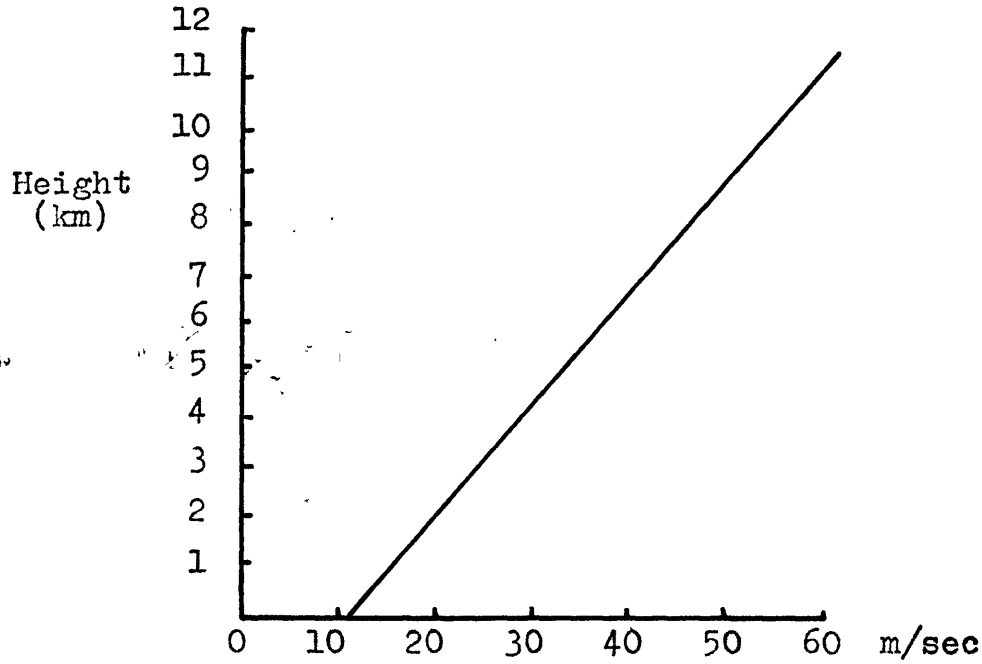

Figure 37. Wind profile at 1300EST, August 28, 1965.

Table 1. Wind Data 0700EST, June 9, 1965
(dd/ff = wind direction/wind speed)*

Level (in mb)	Portland	Albany	Nantucket
1000	No Report	240/02	240/08
850	No Report	270/07	260/10
700	250/13	250/13	270/13
500	260/19	250/16	260/20
400	260/24	250/19	260/28
300	240/29	260/25	260/25
250	240/33	260/23	260/27
200	260/32	270/24	260/30
150	250/20	250/21	260/20
100	260/06	260/09	270/05

Table 2. Wind Data 1900EST, June 9, 1965
(dd/ff = wind direction/wind speed)*

Level (in mb)	Portland	Albany	Nantucket
1000	215/04	No Report	250/10
850	290/10	No Report	260/13
700	280/08	260/12	245/20
500	270/19	260/15	250/21
400	260/22	260/14	250/26
300	250/34	240/28	250/36
200	350/45	240/23	250/36
150	270/17	250/22	250/32
100	265/11	260/11	264/19

*Speeds in meters per second

Table 3. Wind Data 1900EST, June 23, 1965
(dd/ff = wind direction/wind speed)*

Level (in mb)	Portland	Albany	Nantucket
1000	No Report	180/03	216/13
850	225/11	258/20	240/14
700	257/17	253/13	256/08
600	246/17	244/22	232/10
500	236/22	251/19	250/17
400	255/21	245/18	258/18
300	263/22	248/22	271/10
250	267/25	251/27	286/13
200	267/31	242/19	286/13
150	275/17	266/20	302/13
100	279/09	271/06	285/09

Table 4. Wind Data 0700EST, June 24, 1965
(dd/ff = wind direction/wind speed)*

Level (in mb)	Portland	Albany	Nantucket
1000	226/07	No Report	222/09
850	254/10	273/13	242/17
700	247/18	254/19	246/14
600	247/19	263/25	255/17
500	244/22	259/28	240/19
400	236/30	254/24	229/17
300	232/29	242/32	234/13
250	230/32	233/26	235/13
200	238/20	238/25	221/16
150	239/13	248/29	258/11
100	231/35	248/16	237/09

*Speeds in meters per second

Table 5. Wind Data 1300EST, August 28, 1965
(dd/ff = wind direction/wind speed)*

Level (in mb)	Portland	Albany	Nantucket
1000	250/08	No Report	230/09
850	260/16	260/15	250/18
700	250/21	260/17	240/24
500	250/26	250/37	240/26
400	250/31	250/38	240/31
300	230/44	240/43	240/41
250	240/52	240/41	240/48
200	230/50	240/49	240/41
150	240/40	No Report	230/48
100	250/16	240/23	240/19

*Speeds in meters per second

Table 6. Intensity Calibration June 9, 1965

Level	Log Z_e	Rainfall Rate ($mmhr^{-1}$)
1	2.5	1.3
2	2.5	1.3
3	3.2	4.0
4	3.9	10.0
5	4.6	23.0
6	4.9	45.0
7	5.4	91.0
8	5.7	132.0
9	6.0	219.0

Table 7. Intensity Calibration June 23, 1965

Level	Log Z_e	Rainfall Rate ($mmhr^{-1}$)
1	2.4	1.2
2	2.4	1.2
3	3.3	4.0
4	3.8	8.5
5	4.4	20.0
6	4.9	42.0
7	5.4	35.0
8	5.7	141.0
9	6.1	234.0

Table 8. Intensity Calibration June 24, 1965

Level	Log Z_e	Rainfall Rate ($mmhr^{-1}$)
1	2.3	1.0
2	2.9	2.3
3	3.6	6.5
4	4.2	15.0
5	4.6	27.0
6	5.3	69.0
7	5.6	115.0

Table 9. Intensity Calibration August 28, 1965

Level	Log Z_e	Rainfall Rate ($mmhr^{-1}$)
1	2.6	1.5
2	3.2	4.0
3	3.9	10.0
4	4.3	18.0
5	4.9	42.0
6	5.3	75.0
7	5.5	100.0
8	5.7	128.0

Table 10. Characteristics of Cells Case I June 9, 1965

Cell	Cell Duration (minutes)	Cell Motion Direction Speed degrees mph	Location of new cells with respect to old cells	Start of cell EST	End of cell EST
1	28	260/18	First cell	0915	0943
2	26	260/18	right rear	0920	0946
3	30	265/25	right rear	0943	1013

Table 11. Characteristics of Cells Case II June 9. 1965

Cell	Cell Duration (minutes)	Cell Motion Direction Speed degrees mph	Location of new cells with respect to old cells	Start of cell EST	End of cell EST
1	21	280/23	First cell	1837	1858
2	37	280/17	right rear	1845	1922
3	21	260/28	First cell	1857	1918
4	24	250/23	right rear	1903	1927
5	48	280/15	right rear	1905	1953
6	16	265/12	right rear	1913	1929
7	25	275/15	right rear	1922	1947
8	20	270/24	right rear	1947	2007
9	23	275/23	right rear	1947	2010
10	23	265/18	right rear	2007	2030
11	18	270/10	right rear	2013	2031
12	17	270/07	right rear	2031	2048
13	19	270/11	right rear	2031	2050
14	19	300/13	right rear	2047	2106

Table 12. Characteristics of Complexes June 23, 1965

Case	Complex Duration (minutes)	Number of Cells	Cell Lifetime (average)	Cell Area (average)*
III	66	5	18	1.5
IV	26	3	15	1.0
V	75	3	25	1.5

*Cell area in square miles

Table 13. Characteristics of Cells Case III June 23, 1965

Cell	Cell Duration (minutes)	Cell Motion Direction degrees/Speed mph	Location of new cells with respect to old cells	Start of cell EST	End of cell EST
1	22	235/20	First cell	1806	1828
2	19	245/16	forward right	1831	1850
3	19	245/31	forward left	1828	1847
4	11	235/34	forward right	1847	1858
5	17	245/22	forward left	1855	1912

Table 14. Characteristics of Cells Case IV June 23, 1965

Cell	Cell Duration (minutes)	Cell Motion Direction degrees/Speed mph	Location of new cells with respect to old cells	Start of cell EST	End of cell EST
1	14	280/21	First cell	1842	1856
2	16	280/28	left	1846	1902
3	14	300/21	left	1854	1908

Table 15. Characteristics of Cells Case V June 23, 1965

Cell	Cell Duration (minutes)	Cell Motion Direction degrees/Speed mph	Location of new cells with respect to old cells	Start of cell EST	End of cell EST
1	20	250/45	First cell	1806	1926
2	24	250/38	forward	1826	1850
3	31	240/32	forward left	1850	1921

Table 16. Characteristics of Cells Case VI June 24, 1965

Cell	Cell Duration (minutes)	Cell Motion Direction degrees / Speed mph	Location of new cells with respect to old cells	Start of cell EST	End of cell EST
1	22	265/34	First cell	0958	1020
2	20	260/30	First cell	1000	1020
3	21	270/30	First cell	1009	1030
4	16	255/23	First cell	1014	1030
5	11	270/33	First cell	1014	1025
6	23	265/29	forward right	1014	1037
7	21	260/32	right rear	1016	1037
8	16	265/37	right rear	1017	1033
9	15	260/24	First cell	1017	1032
10	20	265/30	First cell	1020	1040
11	16	260/37	right rear	1027	1043
12	21	270/39	First cell	1027	1048
13	31	260/30	left rear	1027	1058
14	25	255/43	right rear	1027	1052
15	25	270/42	First cell	1027	1052
16	28	265/22	forward left	1030	1058
17	25	260/24	right rear	1033	1058
18	26	270/21	right rear	1034	1100
19	--	265/28	forward left	1034	----
20	21	250/21	right rear	1039	1100
21	--	270/29	right rear	1039	----
22	20	260/12	forward	1040	1100
23	15	260/30	forward left	1045	1100
24	07	270/22	forward	1048	1055
25	--	260/25	forward right	1048	----
26	--	265/30	forward left	1052	----
27	--	285/08	forward right	1040	----
28	--	265/30	left rear	1052	----
29	--	265/30	left rear	1057	----
30	--	270/40	right rear	1057	----

Table 17. Characteristics of Cells Case VII August 28, 1965

Cell	Cell Duration (minutes)	Cell Motion Direction degrees / Speed mph	Location of new cells with respect to old cells	Start of cell EST	End of cell EST
1	10	245/36	First cell	1454	1504
2	14	240/30	forward right	1459	1513
3	23	243/39	First cell	1502	1525
4	53	235/37	forward left	1509	1602
5	11	240/38	forward left	1513	1524
6	18	235/37	forward left	1524	1542
7	18	248/40	forward right	1533	1551
8	18	245/36	forward	1551	1609
9	14	248/43	forward right	1600	1614
10	23	236/49	forward left	1602	1625
11	05	230/41	forward right	1612	1617
12	20	245/45	forward right	1617	1637
13	27	240/39	forward	1625	1652

Table 18. Precipitation and Vertical Transports for an Average Cell Assuming Equal Amounts Deposited as Precipitation and Left as Cloud and Neglecting the Complex

Case	Precipitation from average cell (gm)	Mass transport (kg)	Latent heat release (kj)	Momentum transport (kg-m/sec)
I	1.5×10^{10}	6.4×10^{9}	7.5×10^{10}	2.6×10^{10}
II	2.2×10^{11}	9.4×10^{10}	1.1×10^{12}	9.1×10^{11}
III	3.6×10^{10}	1.3×10^{10}	1.8×10^{11}	9.0×10^{10}
IV	5.0×10^{9}	1.8×10^{9}	2.5×10^{10}	1.3×10^{10}
V	3.1×10^{10}	1.1×10^{10}	1.6×10^{11}	7.9×10^{10}
VI	1.9×10^{10}	6.7×10^{9}	9.6×10^{10}	6.5×10^{10}
VII	1.0×10^{11}	3.5×10^{10}	5.0×10^{11}	4.6×10^{11}

Table 19. Precipitation and Vertical Transports for Each Complex

Case	I	II	III	IV	V
I	2.2×10^{11}	2.7×10^{11}	5.8×10^{10}	6.7×10^{11}	5.1×10^{11}
II	3.6×10^{12}	6.7×10^{12}	1.2×10^{12}	1.7×10^{13}	3.9×10^{12}
III	3.9×10^{11}	5.7×10^{11}	1.0×10^{11}	1.4×10^{12}	7.7×10^{11}
IV	5.4×10^{10}	6.9×10^{10}	1.3×10^{10}	1.7×10^{11}	9.2×10^{10}
V	3.3×10^{11}	4.2×10^{11}	7.6×10^{10}	1.0×10^{12}	5.9×10^{11}
VI	1.4×10^{12}	1.9×10^{12}	3.3×10^{11}	4.6×10^{12}	4.3×10^{12}
VII	2.9×10^{12}	4.2×10^{12}	7.4×10^{11}	1.0×10^{13}	9.4×10^{12}

Column Explanations

I. Total precipitation in the complex excluding the cells (gm).

II. Total precipitation in the complex including the cells (gm).

III. Mass transport necessary to produce total precipitation in the complex with no assumption regarding cloud and/or cloud evaporation. (kg).

IV. Latent heat release corresponding to the total observed precipitation in the complex (kj).

V. Downward momentum transport by the complex (kg-m/sec).

Table 20. Average Vertical Velocities (mps) Necessary to Produce Given Amounts of Condensate

Case	I	II	III	IV	V	VI	VII
I	1.9	5.7	7.0	8.9	10.0	11.3	17.1
II	8.1	8.7	10.7	13.4	15.5	17.3	26.1
III	3.0	4.6	5.7	7.2	8.4	9.3	13.8
IV	0.8	1.8	2.2	2.7	3.1	3.6	5.4
V	1.8	4.2	5.0	6.2	7.5	8.5	12.6
VI	2.1	3.9	4.8	6.0	7.0	8.0	11.7
VII	5.8	9.2	11.2	13.9	16.7	18.8	27.6

Column Explanations:

I. Precipitation from an average cell plus an equal amount for cloud and cloud evaporation.

II. Precipitation from the complex.

III. Precipitation from the complex plus an additional 20% for cloud and cloud evaporation.

IV. Precipitation from the complex plus an additional 50% for cloud and cloud evaporation.

V. Precipitation from the complex plus an additional 75% for cloud and cloud evaporation.

VI. Precipitation from the complex plus an equal amount for cloud and cloud evaporation.

VII. Precipitation from the complex plus twice that observed amount for cloud and cloud evaporation.

REFERENCES

Atlas, D., Ed., 1963: Severe Local Storms, Meteorological Monographs, 5, American Meteorological Society, Boston, Mass.

Atlas, D., 1966: The balance level in convective storms, Journal of the Atmospheric Sciences, 23, 635-651.

Austin, J. M., 1948: A note on cumulus growth in a non-saturated environment, Journal of Meteorology, 5, 103-107.

Austin, P. M., 1968: Analysis of small-scale convection in New England, Proc. of the Thirteenth Radar Meteorology Conference, American Meteorological Society, Boston, Mass., 210-215.

Austin, P. M. and S. Geotis, 1960: The radar equation parameters, Proc. of the Eighth Weather Radar Conference, American Meteorological Society, Boston, Mass., 15-22.

Barge, B. L., 1968: Thunderstorm energy budgets from radar data, Proc. of the Thirteenth Radar Meteorology Conference, A.M.S., Boston, Mass., 114-117.

Battan, L. J., 1963: A survey of recent cloud physics research in the Soviet Union, Bulletin of the American Meteorological Society, 44, 757-758.

Boucher, R. H. and R. Wexler, 1961: The motion and predictability of precipitation lines, Journal of Meteorology, 18, 160-171.

Braham, R. R., 1952: The water and energy budget of the thunderstorm and their relation to thunderstorm development, Journal of Meteorology, 9, 227-242.

Byers, H. R., 1942: Nonfrontal thunderstorms, Misc. Rep. No. 3, Univ. of Chicago, Dept. of Meteorology.

Byers, H. R. and R. R. Braham, 1949: The Thunderstorm, United States Dept. of Commerce, Washington, D. C., Govt. Printing Office.

Cochran, H. G., 1961: A numerical description of New England squall lines, S. M. Thesis, Dept. of Met., M.I.T., Cambridge, Mass.

Houghton, H. G. and H. E. Cramer, 1951: A theory of entrainment in convective currents, Journal of Meteorology, 8, 95-102.

Kessler, E., 1967: On the Continuity of Water Substance, Tech, Memo. IERTM - NSSL 33, U. S. Dept. of Commerce, ESSA, 125pp.

Ligda, M. G. H.m 1953: The horizontal motion of small precipitation areas as observed by radar, Weather Radar Research Reprot No. 21, Dept. of Met., M.I.T., Camb., Mass.

Ludlam, F. H., 1963: Severe local storms: a review, Severe Local Storms, Meteorological Monographs, 5, No. 27.

Newton, C. W. and S. Katz, 1958: Movement of large convective rainstorms in relation to winds aloft, Bulletin of the American Meteorological Society, 39, 129-136.

Omotoso, E. A., 1967: Development of the more intense storms in a well organized squall line, M.S. Thesis, Dept. of Met., M.I.T., Camb., Mass.

Starr, V. P. and R. M. White, 1951: A hemispherical study of the atmospheric angular-momentum balance, Q.J.R.M.S., 77, 215-225.

Stem, F. T., 1964: Characteristics of New England thunderstorms viewed on 10 cm radar, S. M. Thesis, Dept. of Met., M.I.T., Camb., Mass.

Swisher, S. D., 1959: Rainfall patterns associated with instability lines in New England, S. M. Thesis, Dept. of Met., M.I.T., Camb., Mass.

Tracton, M. S., 1968: The role of cellular convection within an extratropical cyclone, Proc. of the Thirteenth Radar Meteorology Conference, A.M.S., Boston, Mass., 216-221.